Universität Bremen

OCEAN UNIVERSITY OF CHINA

ALFRED-WEGENER-INSTITUT
HELMHOLTZ-ZENTRUM FÜR POLAR- UND MEERESFORSCHUNG

Master-Thesis

Sino-German Master in Marine Sciences

University of Bremen and Ocean University of China

In cooperation with the Alfred-Wegener-Institute, Helmholtz-Center for Polar- and Marine Research, Bremerhaven

Role of Bicarbonate in the Physiological Response of the Common Shore Crab *Carcinus maenas* to Ocean Acidification

Bastian Maus

Student ID: 2501581

September 2015

First Supervisor: Prof. Dr. Hans-Otto Pörtner

Second Supervisor: PD Dr. Holger Auel

Contents

Abstract

The ongoing increase of carbon dioxide in the atmosphere and in the oceans leads to alternations in the speciation of carbonic acid in the seawater, accompanied by a drop in pH. This phenomenon is termed ocean acidification and animals have been observed to show species-specific physiological adaptations to it. Animals from the intertidal, pre-adapted to variable environmental conditions, are supposed to be more resilient to future ocean acidification due to the high capacities of their ion- and acid-base regulatory mechanisms. Acid-base regulation in a high-CO_2 ocean is effected through the uptake of bicarbonate ions from the surrounding water and supposed to influence an animal's energy budget. The aim of the present study was to identify the role of bicarbonate in influencing haemolymph acid-base- and ion-regulation under elevated CO_2 in an intertidal model species, the shore crab *Carcinus maenas*. Additionally, its potential effects on oxygen consumption (to determine organism metabolic rate) and cardio-vascular performance were of special interest. Individuals were exposed for four weeks to: *0)* present normocapnic conditions *1)* Hyper-capnic conditions, mimicking near-future ocean acidification; *2)* Acidification by a fixed acid, effectively reducing the seawater-concentration of bicarbonate by about 50% and *3)* a combination of the aforementioned two. Standard and routine metabolic rates were measured in intermittent-flow respirometers. The cardio-vascular system and changes in extra- (pH_e) and intracellular pH (pH_i) were observed using *in vivo* magnetic resonance imaging (MRI) and ^{31}P-nuclear magnetic resonance (NMR) spectroscopy. Haemolymph CO_2 parameters and ion composition have been determined through gas-phase- and ion chromatography, respectively.

While metabolic rates and haemolymph flow showed no significant deviations from control values, they were always significantly depressed under reduced seawater bicarbonate, compared to simple ocean acidification conditions. Elevated CO_2 in the water led to an increase of CO_2 in the haemolymph after long-term acclimation, but pH_e and pH_i remained constant due to an active increase of haemolymph HCO_3^- that was not hindered by the availability of bicarbonate from the seawater. This maintenance of acid-base-balance came at the expense of ion homeostasis, possibly caused by shifts in the use of different transporters/exchangers for ion- and acid-base regulation, such as Na^+/H^+ and Cl^-/HCO_3^-, after prolonged exposure. However, neither the acid-base balance nor the concentrations of ions in the haemolymph match the patterns found in metabolic rates and blood flow. Based on findings in other taxa, a direct sensing of the seawater carbonate alkalinity with an effect on oxygen consumption and cardiac activity, involving adenosine as a mediating compound is postulated.

Figures and Tables

Figures

Tables

List of Abbreviations

3-APP	3'-aminopropylphosphonate
α	Solubility coefficient; level of significance
ADP	Adenosin-5'-diphosphate
AEP	2'-aminoethylphosphonat
ANOVA	Analysis of variance
ATP	Adenosin-5'-triphosphate
$\beta(CO_2)_w$	CO_2 capacitance coefficient in water
$[B]_T$	Total boron concentration
bpm	beats per minute
°C	Degree Celsius
c	Concentration
Ca^{2+}	Calcium ion
Cl^-	Chloride ion
CO_2	Carbon dioxide
CO_3^{2-}	Carbonate ion
δ	Chemical shift
FLASH	Fast low angle shot
g	Gramm
GABA	Gamma-aminobutyric acid
H^+	Hydrogen ion / proton
h	Hour(s)
HCO_3^-	Hydrogen carbonate / bicarbonate ion
H_2CO_3	Carbonic acid
H_2O	(Distilled) water
HCl	Hydrochloric acid
I	Ionic strength
K^+	Potassium ion
L	Liter
M	Molar (mol/L)
m	Meter
m	Mass
Mg^{2+}	Magnesium ion
min	Minute(s)
mol	Mol
$\dot{M}O_2$	Metabolic- / respiration rate
MRI	Magnetic resonance imaging
n	Amount of substance; group size
Na^+	Sodium ion
NaOH	Sodium hydroxide
NH_4^+	Ammonium ion
NMR	Nuclear magnetic resonance
O_2	Oxygen
P	Phosphorous
P	(Partial-) pressure; probability
$P(CO_2)_e$	Partial pressure of CO_2 in haemolymph
$P(CO_2)_w$	Partial pressure of CO_2 in seawater
P_i	Inorganic phosphate
pH	$-\log_{10}[H^+]$
pH_e	Extracellular pH
pH_i	Intracellular pH
pH_w	Sea water pH (free scale)
pK_a	$-\log_{10}$ of dissociation constant in an acid-base equilibrium
pK_a'''	pK_a under defined conditions
PLA	Phospho-L-arginine
PSU	Practical salinity unit
ppm	Parts per million
RARE	Rapid acquisition with relaxation enhancement
RCP	Representative concentration pathway
RMR	Routine metabolic rate
S	Seawater salinity
SMR	Standard metabolic rate
SO_4^{2-}	Sulfate ion
T	Tesla
T	Temperature
t	Time
V	Volume
w_f	Wet weight / fresh weight

1. Introduction

1.1 Anthropogenic ocean acidification and its effect on animal physiology

The increasing rates of fossil-fuel-burning and deforestation over the last centuries lead to increasing atmospheric concentrations of carbon dioxide (CO_2; Doney et al. 2009; IPCC 2013). The atmospheric increase has been buffered by the uptake of CO_2 by the oceans, which effectively act as a sink (Sabine & Feely 2007). This leads to alterations of the carbonate chemistry of seawater, according to the following reactions:

$$CO_2 + H_2O \leftrightarrow H_2CO_3 \overset{aq.}{\leftrightarrow} H^+ + HCO_3^- \quad [1]$$

$$HCO_3^- \overset{aq.}{\leftrightarrow} H^+ + CO_3^{2-} \quad [2]$$

Hypercapnia, denominating an increase in ambient CO_2 ($P(CO_2)$), will lead to an increase in $[H^+]$ and thus to a reduction of seawater pH, termed ocean acidification (Doney et al. 2009). The representative concentration pathways (RCPs) project atmospheric CO_2-concentrations between 400 ppm and 1000 ppm by the year 2100 (Meinhausen et al. 2011), leading to an average drop in ocean pH by 0.4 – 0.5 below present (Wittmann & Pörtner 2013). Generally, an acidification due to an input of CO_2 in seawater will slightly increase the concentration of HCO_3^- and decrease that of CO_3^{2-}. Together with these alternations in the concentrations of the dissolved inorganic carbon species and a drop in pH_w, ocean acidification will cause physiological responses of single species and thus of the ecosystem itself.

The investigation of the responses to hypercapnia in energy metabolism, acid-base regulation or narrowing of the thermal tolerance window and has been the subject of several studies (for reviews, see Whiteley 2011; Wittmann & Pörtner 2013). Determined through short- or long-term exposure to various degrees of hypercapnia, it became obvious that an increased $P(CO_2)$ requires adaptations at various organizational levels – from molecular to systemic. The capacities of these adaptations define the sensitivity of the individual to ocean acidification. Under elevated $P(CO_2)_w$, more CO_2 diffuses across body epithelia and equilibrates between extra- and intracellular compartments causing a more acidic state (Fabry et al. 2008). If uncompensated, drops in extra- (pH_e) and/or intracellular pH (pH_i) have been shown to affect metabolic rates, expressed as the rate of oxygen consumption ($\dot{M}O_2$). Metabolic depression, as witnessed in many studies (Reipschläger & Pörtner 1996; Michaelidis et al. 2005; Small et al. 2010) has been reported, as well as no changes (Gutowska et al. 2008; Lannig et al. 2010) or even an increase in the metabolic rates (Thomsen & Melzner 2010) across a range of animal

species. The lack of a clear pattern seems to indicate that responses in energy metabolism to ocean acidification differ on a species-level (Melzner et al. 2009; Whiteley 2011). However, unifying principles of effects and their variability need to be identified before conclusions can be drawn.

Regulatory processes leading to a new physiological steady-state may cause reallocations of energy to different energy consuming processes such as ion regulation and protein biosynthesis. The enhanced activity of a given mechanism could simply lead to increased energy demands. More extreme stress might not be completely compensated and an animal can then enter a metabolically depressed state with $\dot{M}O_2$ below standard rates (see below) to conserve energy. This is a way to prolong survival time until conditions return to the optimum (Guppy & Withers 1999, after Lannig et al. 2010). It remains to be seen, what the exact triggers for these responses are and to what extent endo- or exogenous drivers interact.

Usually, compensation of an increase in $[H^+]$ in body fluids is effected by ion-exchange mechanisms, causing shifts between the different components of the carbonate system. The capacities of pH regulation may play a key role in resilience to hypercapnia: An early study by Reipschläger & Pörtner (1996) on the polychaete *Sipunculus nudus* showed that for this species, drops in pH_e lead to a reduced aerobic metabolism. Later, they concluded that shifts in the use of different H^+ transporting mechanisms from those with higher energy demand (Na^+/K^+-ATPase and Na^+/H^+ exchange) to those with a lower energy demand (Na^+-dependent Cl^-/HCO_3^- exchange) could effectively save energy for the animal and thus be responsible for reduced metabolic rates (Pörtner et al. 1998; 2000). Respiration rates in the velvet swimming crab *Necora puber* were depressed after 30 days of exposure to hypercapnia, despite a fully compensated pH_e (Small et al. 2010). As mentioned above, metabolic depression in combination with an uncompensated drop of pH_e was also found for some bivalves (Michaelidis et al. 2005). The blue mussel *Mytilus edulis*, on the other hand could be identified to increase its metabolic rate under more moderate levels of hypercapnia (Thomsen & Melzner 2010; Stapp et al. 2014), similar to cephalopods like *Sepia officinalis*: Even though an acidosis of their body fluids has not been fully compensated for, metabolic rates remained stable. Preadaptation to a high level of motor activity seems to be involved in setting the capacities of their compensatory mechanisms high, such as ion-transport- and acid-base regulatory systems. Combined, these capacities result in a high tolerance to hypercapnia in *S. officinalis* (Gutowska et al. 2008). pH_e may not be the only trigger of metabolic depression as suggested by the role of adenosine in *S. nudus* (Reipschläger et al. 1997). In the present study, the interrela-

tionships between acid-base regulation, ion regulation and energy metabolism in response to ocean acidification should be investigated, with the aim to identify possible exo- or endogenous triggers for a metabolic depression. Special attention is paid to modulations of these responses due to a reduced availability of bicarbonate from the seawater, since bicarbonate-uptake is known to play an important role in the compensation for a hypercapnic acidosis (see below).

1.2 The shore crab, *Carcinus maenas*

1.2.1 Morphology and Ecology

Carcinus maenas (Linnaeus 1758) is a widely spread and well-studied species of decapod, brachyuran crustaceans. The carapace rarely extends beyond 10 cm in width, displaying various shades of green, brown, orange and red coloring. Typical for a brachyuran, its abdomen is greatly reduced and folded under the cephalothorax. Even though it is recognized as a member of the Portunidae – the swimming crabs – it almost lacks the flattened dactylus at the last pair of walking legs and thus any swimming capabilities (Crothers 1967, fig. 1). Due to its active, predatory lifestyle in the intertidal, the species already experiences extreme values of various environmental parameters (T, S, $P(O_2)$, $P(CO_2)$) and is able to tolerate them in its everyday life. Based on the associated pre-adaptations of e.g. ion regulation mechanisms, the shore crab can be studied with the aim to understand general and long-term effects of hypercapnia on its physiology (Pörtner et al. 2004; Whiteley 2011).

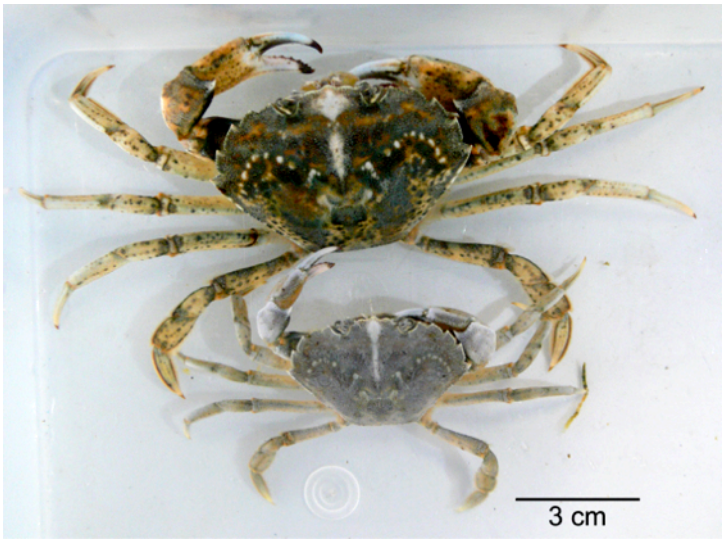

Fig. 1. Dorsal view of two *C. maenas* (experimental animals 1.5 (top) and 1.6). Individuals represent the range in body size of the experimental animals. The white dots on the carapace are known to be the attachment points of the muscles. The differences in coloring are related to age and molting cycle. Note the absence of a flattened dactylus at the fifth walking leg.

The fact that it has spread far over the northern hemisphere indicates *C. maenas*' capability of successfully adapting to changing conditions over longer timescales (fig. 2; Aronson et al. 2014; Tepolt & Somero 2014). It has thus become one of the most extensively studied intertidal crabs in the world (Reid et al. 1997).

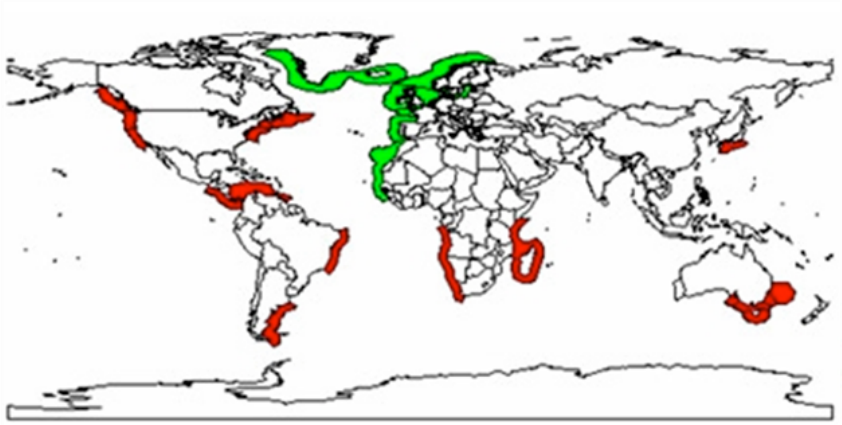

Fig. 2. Global distribution of *C. maenas.* Green: native range; Red: invasive range. Source: http://invasions.si.edu

Males may grow larger, with relatively larger chelae and display a more aggressive behavior when disturbed. Their abdomen is triangular and has five segments, compared to the more broad and rounded abdomen with seven segments of the adult females (Crothers 1967). Aside from these subtle morphological and behavioral differences, only male *C. maenas* are known to have 2-aminoethylphosphonate (AEP) in their haemolymph, which can be detected e.g. as a distinct peak in *in vivo* ^{31}P-NMR spectra (Kleps et al. 2007). This can serve to verify the sex, determined in the individuals according to morphological criteria. At least two distinct colorings of wild crabs can be observed, referring to their two other common names: green crab and red crab. It has been found that these states reflect the molting stage: All postmolt crabs are green carbs but during prolonged intermolt, their color changes to orange and finally to a more reddish color (McGaw et al. 1992). Red crabs tend to have more epibionts and shell fractures than the green ones but are more competitive in fights for food or sex partners (Kaiser et al. 1990).

1.2.2 Circulatory and respiratory systems

Typical for arthropods, *C. maenas* has an open circulatory system, though a few arterial "blood-vessels" can be identified. The haemolymph, which provides most of the functions of vertebrate blood, is pumped from the heart through three non-muscular arteria: the aorta in anterior direction, the *arteria abdominalis dorsalis* that reaches far into the abdomen and the *arteria sternalis*, reaching to the ventral bases of the walking legs (fig. 3; Crothers 1967; Storch & Welsch 2009). *Carcinus maenas* has been found to sustain an unchanged heart rate

under aerial exposure. Despite drops in its haemolymph $P(O_2)$, it does not go into bradycardia when exposed to air, like for example the subtidal velvet crab *Necora puber* (Johnson & Uglow 1985). This adaptation is associated with *C. maenas*' intertidal habitat (Taylor & Butler 1978). Its highly potent cardiac system is therefore of potential interest in studies concerning the overall performance and energy budget, to determine those factors that may actually interfere with cardio-vascular activity. Energy budget here is defined as the sum of the energy turnover of aerobic, metabolic processes.

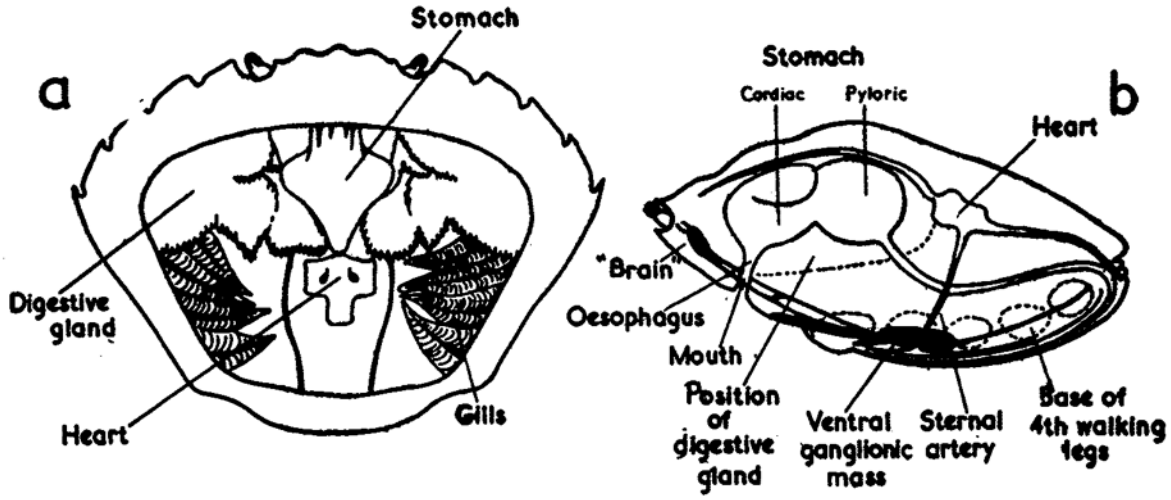

Fig. 3. Schematics of the internal organs of *C. maenas*. A) Dorsal (coronal) view The digestive gland is also known as mid-gut gland. **B)** Lateral (axial) view, including the three arteria mentioned in the text. Taken from Crothers (1967).

Gas exchange and part of the ion exchange with the surrounding water is effected through nine pairs of gills. The gills are encased in the cephalothorax and connected to the surrounding water via six openings. The oxygen-carrying molecule in the haemolymph of *C. maenas* is haemocyanin, which has a relatively low oxygen binding capacity, compared to vertebrate haemoglobins (Crothers 1967) but still shows a typical Bohr-effect (Truchot 1975). Phases without detectable heart beat and gill ventilation of the shore crab are reported in undisturbed crabs. The phases of extremely low values in heart beat are much shorter (seconds to 1 min) than those in respiration, which can last for hours (Uglow 1973; Klein Breteler 1975; Cumberlidge & Uglow 1977).

1.3 Metabolic rate and respirometry

Metabolic rate is defined as the heat production of catabolic processes (Fry 1971), which include both aerobic and anaerobic processes. Oxygen consumption is most often taken as a proxy for energy demand and metabolic rate, since aerobic metabolism is the only way to sustain animal life for a longer period of time. Aside from oxidative phosphorylation, oxygen

may also be consumed in other cellular reactions, but these account for just 10-15% of the total oxygen consumption e.g. in rat hepatocytes (Brand 1990; Nobes et al. 1990). Especially whole-animal metabolic rate is usually equivalent to respiration- or oxygen-uptake rate, even though the initial concept of the two is still different. On the whole-organism level, respiration rate can be regarded as the integral of all energy consuming processes. This may limit its qualitative significance, as depressed metabolic rates in one process or tissue may be overlapped by increases in another, totaling in more-or-less unchanged whole-animal metabolic rates. Still, it remains a valuable measure for the physiological state of an animal (Fry 1971).

Various levels of metabolic rate have received attention in physiological studies, ranging from minimum to maximum oxygen uptake in order to determine (maximum) aerobic scope of an animal, defined as the difference between the two or factorial aerobic scope, defined as $\dot{M}O_{2max}/\dot{M}O_{2min}$. Calculation of both parameters can give insight into the absolute and proportional capacities of aerobic metabolism to increase over basal metabolism. The minimum respiration rate that can be sustained over an extended period of time without additional sources of energy use in a post-absorptive, resting animal is defined as standard metabolic rate (SMR). It comprises the energy- or oxygen demand of resting cells and of the mechanisms maintaining cellular functioning (Fry 1971; Brand 1990). In contrast, routine metabolic rate (RMR) is defined as and caused by spontaneous, unforced but somewhat restricted activity, determined from a time series of respiration rates (Fry 1971; Klein Breteler 1975).

In this experiment, metabolic rate of the shore crab *C. maenas* shall be measured under differently acidified seawater, in order to determine the effects of ocean acidification on the whole animal energy budget, which can be estimated through the oxygen uptake. Measurements of undisturbed, unrestrained crabs for 48 h will yield values of standard- and routine metabolic rates, so any influence on – for example the relative proportion of time periods when animals use SMR and RMR and their magnitudes – can also be assessed.

1.4 Acid-base and ionic regulation in crustaceans

In all species, the uptake of HCO_3^- from the surrounding water has been reported to play a vital role in the response to hypercapnia, even during prolonged exposure (e.g. Pörtner et al. 1998 for *S. nudus* and Gutowska et al. 2008 for *S. officinalis*; for *C. maenas* and other crustaceans: Truchot 1979; Spicer et al. 2007; Whitely 2011; Appelhans et al. 2012). The uptake of bicarbonate or the excretion of protons are supposed to be the most important adaptations to counter acidification, since similar mechanisms are known on a cellular level in tissues with

high energy turn-over, e.g. in muscle cells: In order to reduce changes in pH_i due to the dissociation of metabolic CO_2 to HCO_3^- and H^+, the protons are buffered by intracellular buffers such as amino-acid side-chains. Excess HCO_3^- is transported to the extracellular space and pH_i is kept constant to ensure optimal enzyme activity (Eckert et al. 2002). The respiratory acidosis in the extracellular compartment caused by an elevation of $P(CO_2)_w$ and consequently $P(CO_2)_e$, is partly buffered by non-bicarbonate buffers, such as haemocyanin. Ion exchange processes (see below) then actively set new steady-state values for pH_e, e.g. through the active uptake of bicarbonate from the seawater. Therefore, the availability of bicarbonate from the surrounding medium or other sources (such as the shell) is believed to affect the degree and extent of pH compensation (Spicer et al. 2007). A sheer rise in $P(CO_2)$ not only leads to a drop in pH, but also to a passive increase in $[HCO_3^-]$. This increase is more pronounced in compartments with a high non-bicarbonate buffering capacity, like the intracellular space. Thus pH_i is more stable than pH_e, which is in turn more stable than seawater pH, if subjected to the same rise in $P(CO_2)$, owing to a decline of non-bicarbonate buffers in that order (Pörtner et al. 2004).

Acid-base regulation in aquatic organisms is tightly coupled to ion regulation, since exchange processes of acid or base equivalents (such as HCO_3^-) with the environment always include an ionic compound to balance electric charges and osmolarity. Efficient iono-regulators are thus known to be efficient acid-base regulators (Whiteley 2011). Meta-analyses have shown that crustaceans have a lower sensitivity than other phyla to projected ocean acidification according to RCP6 and RCP8.5 leading to atmospheric concentrations of 670 and 936 ppm CO_2 by the year 2100 respectively (Wittmann & Pörtner 2013). One reason could be their high degree of pre-adaptation to coastal and shallow water habitats and the associated fluctuation of abiotic parameters. Especially for *C. maenas*, being stranded in tidal pools and exposure to progressive hypoxia, hypercapnia and changes in salinity is not uncommon, so the species' regulatory mechanisms have likely evolved a high capacity to adjust to these conditions. The higher sensitivity of deep-sea crustaceans to similar degrees of environmental hypercapnia is expressed by their reduced capacity of extracellular acid-base regulation in line with an energy saving mode of life at constant and cold environmental conditions (Pane & Barry 2007).

The importance of studying the influences of the interrelated dependencies of the seawater carbonate system is stressed by Truchot (1981; 1984), as a reduction in total alkalinity at normocapnia (equivalent to a reduction in $[HCO_3^-]_w$) caused an uncompensated respiratory acidosis in the haemolymph of *C. maenas*. At simultaneously reduced salinity, this state was found to be transitory, indicating a strong connection between ion- and acid-base regulation,

independent of $P(CO_2)_w$. Interestingly, the haemolymph acid-base balance of crabs acutely exposed to environmental hypercapnia was not differently affected by reduced or normal seawater alkalinity. The way how the seawater is acidified is supposed to have a significant effect on animal physiology, as it has been shown for the Japanese sea bream *Pagrus major*: CO_2-enriched water was found to be far more toxic to early life stages than HCl (a fixed acid) acidified water at the same pH_w (Ishimatsu et al. 2004).

A new steady-state with high levels of $[HCO_3^-]_e$, set by electro-neutral ion exchange processes, reduces the importance of passive non-bicarbonate buffering in the response to hypercapnia (Whiteley 2011). Since ion-regulation often is an energy-consuming process, working against concentration gradients, reallocation of energy within cells, tissues and whole organisms may be necessary under hypercapnia. The two processes of acid-base- and ion-regulation can therefore only be studied together. Even though continuous accumulation of bicarbonate from whatever source may compensate acidification in the body fluids, an upper limit in its accumulation is hypothesized at which a terminal compromise between acid-base- and ion balance is reached (Cameron & Iwama 1989). Analyzing the ionic composition of the haemolymph will reveal whether hypercapnia and/or the availability of single ions will have any effect on their total and relative concentrations, thus possibly indicating shifts in ion exchange processes, contributing to acid-base regulation.

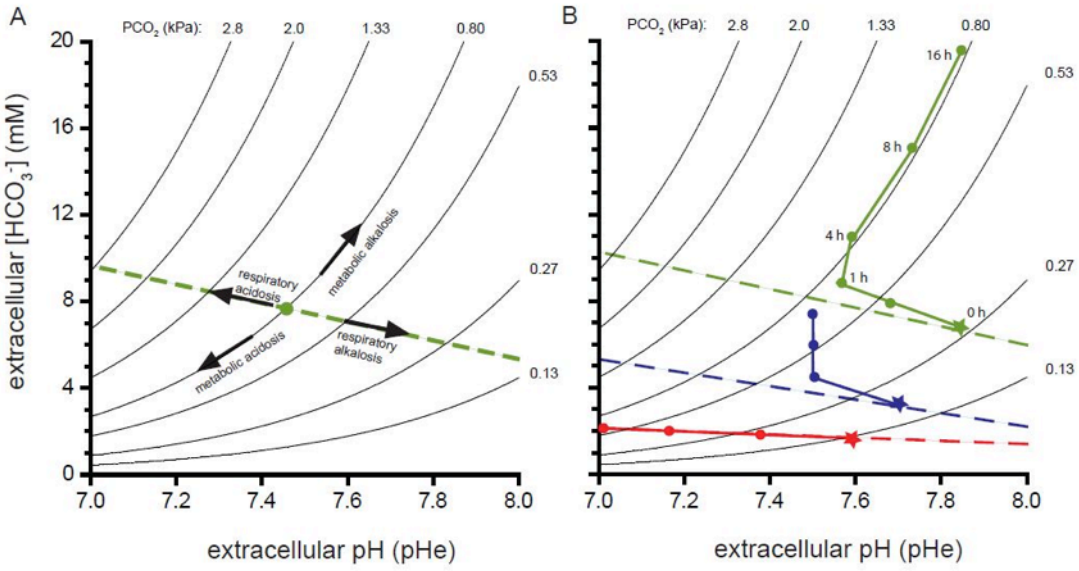

Fig. 4. Exemplary pH/bicarbonate diagrams. A) Schematic illustration of a non-bicarbonate buffer line (dashed green line). Arrows indicate changes in $P(CO_2)$ and $[HCO_3^-]$ during respiratory acidosis/alkalosis and metabolic acidosis/alkalosis. **B)** Extracellular fluids of three different hypothetical organisms subjected to 0.5 kPa (5000 ppm) environmental hypercapnia. Red symbols: No active accumulation of bicarbonate in the extracellular space to compensate pH, pH follows the non-bicarbonate buffer line. Blue symbols, green symbols: partial/full pH compensation through active bicarbonate accumulation. Stars indicate control parameters, numbers indicate exposure time (*h* = hours, hypothetical time course) to elevated $P(CO_2)$. Taken from Melzner et al. (2009).

The way pH_e responds to any disturbances and how efficient the accumulation of HCO_3^- is to adjust pH_e to a new steady state can be seen when plotting $[HCO_3^-]_e$ against pH_e and $P(CO_2)_e$ (fig. 4). Regulation of pH_e, against an elevated $P(CO_2)_e$ (respiratory acidosis) is effected by an increase of $[HCO_3^-]_e$ beyond the physico-chemical dissociation of H_2CO_3, which is symbolized by the slope of the non-bicarbonate buffer line.

Ion-regulation and thus acid-base regulation is supposed to take a considerable share in standard metabolism as maintenance and adjustments of the ion composition in its body fluids is crucial for the organism. Depending on the environmental conditions, the activity of Na^+/K^+-ATPase alone is taking up to 40% of the total energy expenditure (Whiteley 2011). The importance of carbonic anhydrase and the basolateral Na^+/K^+-ATPase for acid-base regulation is stressed in the posterior gills of *C. maenas* (Siebers et al. 1994; fig. 5). But since V-type H^+-ATPases were found to be more abundant in the anterior gills, no clear segregation of a localized acid-base regulation predominated by a certain pair of gills or ion exchange process should be made (Weihrauch et al. 2001; Fehsenfeld & Weihrauch 2013). Generally, ion exchange in the gills is driven by gradients of Na^+, built up through the primary active basolateral Na^+/K^+-ATPase. Lower intracellular concentrations of Na^+ will lead to an uptake from

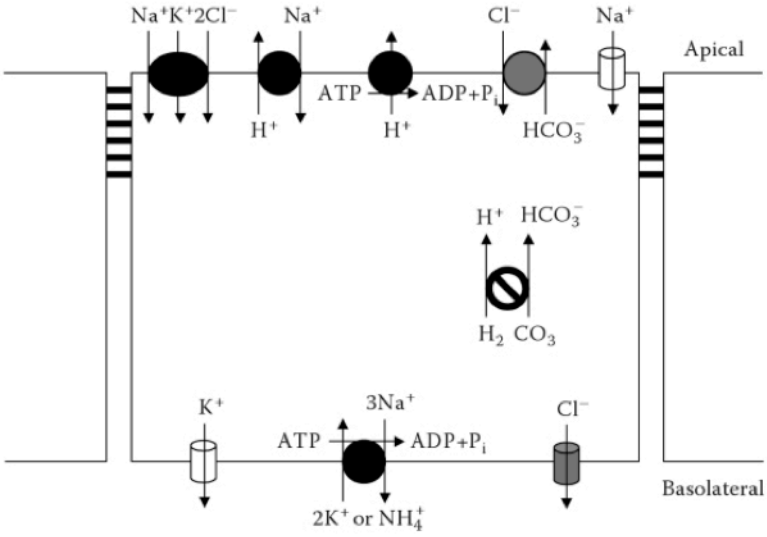

Fig. 5. Hypothetical working model of NaCl related ion regulation across gill epithal cells of hyperosmoregulating crustaceans, like *C. maenas,* based on numerous physiological, ultrastructural and molecular studies. Subcellular localization studies have been accomplished for only a few of the transporters. Basolateral (facing the haemolymph) Na^+/K^+-ATPase is thought to generate an electrochemical potential that energizes apical (facing the seawater) transport processes, including epithelial Na^+ channels, Na^+/H^+ exchangers and $Na^+/K^+/2Cl^-$ co-transporters. Apical Cl^-/HCO_3^- exchangers may mediate Cl^- uptake along with $Na^+/K^+/2Cl^-$ co-transporters. Note that transporters can operate in both directions and their role in HCO_3^- uptake is discussed in the text. Intracellular HCO_3^- levels are mediated by the action of soluble carbonic anhydrase. V-type H^+-ATPase may be responsible for the active excretion of excess protons. Basolateral transport of Cl^- and K^+ may be mediated by respective channels. Transporters represented in gray have been identified at the molecular level in crustacean gills; In addition, gene expression data are available for those represented in black. Taken from Charmantier et al. (2009).

the seawater through electroneutral, secondary active $Na^+/K^+/2Cl^-$ co-transporters and Na^+/H^+ antiporters. The exchange of Cl^- for HCO_3^- is driven by these combined activities of the Na^+/K^+-ATPase and the $Na^+/K^+/2Cl^-$ co-transporter and, in connection to the activity of intracellular carbonic anhydrase, is supposed to effectively mediate the compensation for a hypercapnic acidosis. It should be stressed again, that shifts from more energy demanding ion exchanges (involving ATPases) to those with lower energetic costs (electroneutral exchanges) in response to a drop in pH_e are supposed to lead to metabolic depressions (Pörtner et al. 1998; 2000).

1.5 Aim of the study and working hypotheses

With seawater bicarbonate supposed to be a major contributing factor to the acid-base regulation of marine species, the present study aims to investigate if the regulation of extracellular and intracellular pH is effective under hypercapnic conditions and if it is dependent on the availability of seawater bicarbonate. In addition, it shall be investigated if this regulation has any effects on the energy demand of the whole animal, thereby elucidating the role of extracellular pH. Animals exposed to hypercapnic conditions (high $P(CO_2)_w$) at normal $[HCO_3^-]_w$ will be compared to those at high $P(CO_2)_w$ and low $[HCO_3^-]_w$ in order to determine the role of bicarbonate and pH_e in the response of *C. maenas* to hypercapnia. Whether any effects are induced by a reduced availability of bicarbonate alone is assessed in one group exposed to normocapnia and an acidification by a fixed acid, effectively reducing $[HCO_3^-]_w$.

Acid-base regulation is essential for the maintenance of optimal functioning of proteins, as well as for the oxygen affinity of haemocyanin (Truchot 1975; Eckert et al. 2002). Any changes in the associated metabolic costs – also visible in cardio-vascular activity – may reflect the strain put on the animal. An increased haemolymph flow rate will affect the exchange rates of metabolites and respiratory gases with the tissues and with the environment, since a steeper concentration gradient is maintained, enhancing diffusive transport (Dejours et al. 1970; Stegen & Grieshaber 2001). Because acid-base regulation is supposed to be achieved by ion exchange processes, the determination of the concentrations of ions in the haemolymph will reveal the compromise between ion- or pH homeostasis as well as to give hints on possible changes in the way pH_e is regulated. In case pH_i disturbances are compensated for under the experimental conditions and the disturbances of pH_e are not, this will also change the ion composition of the haemolymph. It shall be evaluated, if reduced availability of seawater bicarbonate can be compensated for by other ion exchange processes to possibly regulate pH_i and pH_e. The following hypotheses are going to be tested:

- Ocean acidification simulated by an increase of seawater $P(CO_2)$ (hypercapnia) leads to an increase of internal $P(CO_2)$ in the shore crab *C. maenas*. Decreasing pH, especially in the extracellular compartment is compensated for by an increase of $[HCO_3^-]_e$ after four weeks of exposure. pH_e compensation is paralleled by shifts in ion homeostasis due to the interdependencies between acid-base and ion regulation.
- The whole animal oxygen uptake at standard and routine levels, cardiac activity and the haemolymph ion concentrations are affected by the exposure to hypercapnia. A drop in pH_e is supposed to lead to metabolic depressions.
- A reduced availability of bicarbonate in the seawater will reduce the internal levels of bicarbonate and thus reduce the ability to balance pH_e against an increasing $P(CO_2)$. This will lead to changes in metabolic rate, cardiac activity and/or ion status, as detected from the ion composition of the haemolymph, when compared to hypercapnia at control bicarbonate concentrations.
- The manipulation of water bicarbonate levels and the resulting shifts in the set points of ion and acid-base regulation in relation to metabolic activities will provide further insight into the role of pH and other relevant parameters under ocean acidification.

2. Materials and Methods

2.1 Collection and incubation of experimental animals

Individuals of the common shore crab, *Carcinus maenas*, were taken from bycatch of shrimp trawls at the backbarrier tidal flats of the island of Spiekeroog (North Sea, north-western Germany, 53°44'27.8"N 7°44'35.7"E) in October 2014. They were kept in re-circulating seawater aquaria at the facilities of the Alfred-Wegener-Institute, Bremerhaven at 8°C, $S \approx 33$ until the beginning of the incubation in March 2015. Animals were fed twice a week *ad libitum* with frozen cockles. Excess food and feces was regularly removed from the aquaria. The fresh weight of the crabs determined after the respiration experiments ranged from 21 to 66 g.

The incubation conditions are summarized in tab. 1. Aside from a control group at ambient $P(CO_2)_w$, group 1 was exposed to increased CO_2-levels, resembling typical ocean acidification conditions. In the water for group 2, pH_w and thus $[HCO_3^-]_w$ were lowered by the addition of 25% HCl. Group 3 was kept at high $P(CO_2)_w$ with the additional reduction of $[HCO_3^-]_w$ through HCl. The amount of HCl was intended to add 1.2 mmol of protons to the water, in order to reduce the $[HCO_3^-]_w$ by approximately that amount (verified by measurements as described in *2.2 Monitoring of water parameters*). For the calculation of the necessary amount of HCl, refer to the calculations in the appendix.

Tab. 1. Experimental groups with desired conditions. Group size indicates number of animals at the beginning of the incubation. Values for pH_w are measured means from fig. A1D (see appendix). The incubation temperature for all groups was 8°C.

Group	Group size / *n*	$P(CO_2)_w$ / ppm	$[HCO_3^-]_w$ / mM	pH_w
control	8	390	2.3	8.12
1	7	1800	2.3	7.50
2	7	390	1.1	7.85
3	7	1800	1.1	7.19

Animals were kept in 50 L seawater aquaria in a temperature controlled room (7 – 8°C, leading to a constant T_w of 8°C) and exposed to the respective conditions for four weeks prior to any experiments. Each crab was kept in individual, wired cages during the incubation. The aquaria were connected to a circulating supply of 790 L natural seawater for each group. The incubation system per group consisted of a 500 L main tank, a header tank, two aquaria and an overflow basin (fig. 6). The water of the control group and group 2 was aerated with compressed air (ambient $P(CO_2)$), while groups 1 and 3 were aerated with an air/CO_2 mix, set by a mass-flow regulated gas-mixing device (HTK Hamburg GmbH, Germany). The volume of the 500 L main tanks was exchanged with new seawater, prepared for the respective conditions, once per week for every group.

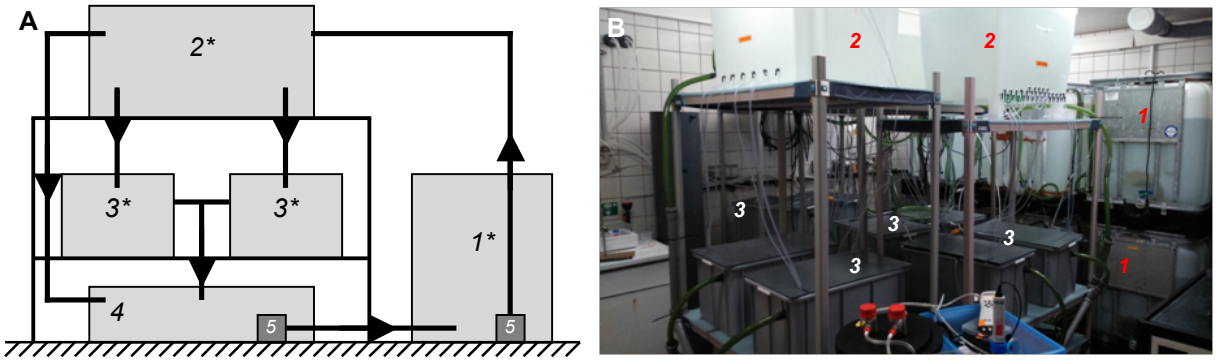

Fig. 6. Incubation setup. 1) Main tank; 2) Header tank; 3) Incubation aquaria; 4) Overflow basin; 5) Water pumps. **A)** Schematic design. One setup like this was chosen for each group. The arrows indicate water flow. Asterisks denote where the water is aerated with the respective gas-mix to achieve $P(CO_2)_w$ given in tab. 1. **B)** Photograph of the incubation room. The main tanks, together with the reserve tanks are stacked in the background. The two header tanks of groups 1 and 3 are visible on top of the respective racks. The solid covers on each of the incubation aquaria were necessary to prevent CO_2 exchange with the ambient air.

2.2 Monitoring of water parameters

Water temperature, salinity, $P(CO_2)_w$ and pH_w (free scale) were measured once a week in each aquarium, as well as in the supply tanks for the *in vivo* measurements before the insertion of the animals (see below). Temperature and salinity were measured directly in the aquaria with a conductivity meter (LF197, WTW, Weilheim, Germany). $P(CO_2)_w$ was determined from the gas phase of the seawater with the help of a combined carbon dioxide probe (CARBOCAP GMP343, Vaisala, Helsinki, Finland) and carbon dioxide meter (CARBOCAP GM70, Vaisala). The pH-meter (pH3310, WTW, Weilheim) was calibrated with NIST buffers (pH 6.865 and 9.180) at the apparent incubation temperature. The pH of the aquaria was determined in 50 mL subsamples covered with parafilm to prevent gas exchange. The values were then transferred to the free scale, with corrections for temperature, ionic strength and a reference buffer-pH in artificial seawater (Waters & Millero 2013), as recommended by Riebesell et al. (2010). $[HCO_3^-]_w$ was then calculated from these data through the "CO2Sys" macro for Microsoft Excel (v2.1, Pierrot et al. 2006), with values for K_1 and K_2 from Millero (2010), KSO_4 from Dickson (1990) and $[B]_T$ from Uppström (1974).

2.3 Respirometry

The respiration rate in aquatic animals can be quantified by measuring the decline of oxygen in a constant volume of water over a period of time. Nowadays, continuous online measurements can be done with fiber-optic sensors (optodes) or galvanic oxygen electrodes. Various designs of respirometers have been developed to ensure well-controlled experimental condi-

tions: While closed respirometers possibly allow for very accurate measurements of the consumption of oxygen, they do not allow for water exchange from the outside, which limits the total duration of one animal-experiment (Taylor & Butler 1973; Klein Breteler 1975).

In case SMR needs to be determined, requiring prolonged respiration measurements, flow-through or intermittent flow respirometers are recommended. Flow-through respirometers are characterized by a constant stream of water through the chamber, where the oxygen consumption is calculated from the difference of $[O_2]$ between in- and outflowing water. The advantage of long measurements comes at the expense of a low resolution in detectable oxygen consumption due to the constant mixing of residual water with the inflowing high-$P(O_2)$ water and a high technical effort (Steffensen 1989; Titulaer 1991). To address these issues, intermittent-flow respirometers incorporate a periodic – and preferably automated – switch from closed circulation (measurement) to open-circulation (flushing with surrounding medium). This design thus benefits from the higher accuracy of a closed respirometer, while a depletion of oxygen or an accumulation of metabolic excretory products is greatly reduced during the open exchange periods (Steffensen 1989) and it therefore was chosen in this experiment.

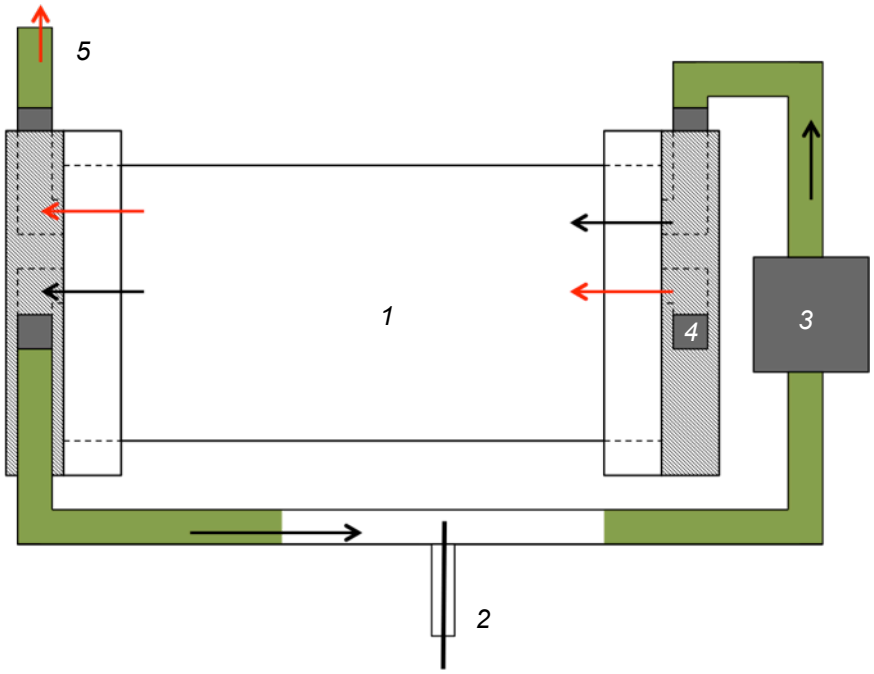

Fig. 7. Schematic design of a respiration chamber. Red arrows show the water flow of the open circulation during flushing, black arrows show the flow during closed measurement circulation. 1) Animal chamber; 2) Tip of fiberglass optode, could be detached from tubing for calibration; 3) Circulation pump; 4) Inflow from the flushing pump (not shown); 5) Outflow during flushing, placed above the water surface.

For measurements of the individual oxygen consumption rates ($\dot{M}O_2$), single specimens of *C. maenas* were placed in a respiration chamber with $V_{chamber}$ = 1720 mL (fig. 7), which in turn was submerged in a basin filled with 40 L seawater (fig. 8). The basin was covered with black

plastic foil to reduce gas exchange with ambient air as well as to prevent visual stress for the crabs. The whole system was set up in the same air-conditioned room as the incubation at a water temperature of 8 ± 1°C.

Fig. 8. Arrangement of the respirometers in the basin.

To ensure that the basin water has the appropriate $P(CO_2)_w$, it was permanently aerated with the respective air-CO_2-mix. For measurements of groups 2 and 3, HCl was added prior to the insertion of the animals. Mechanic clock timers controlled the periodic activation of one flush pump per respirometer. This open circulation lasted for 15 min every hour at a rate of 300 L/h. The closed measurement-circulation at 490 L/h was continuously active (Eheim aquarium pumps, Deizisau, Germany). The oxygen-content as percent of air-saturation was measured continuously with a fiberglass optode, an optical oxygen meter (FIBOX 3; PreSens, Regensburg, Germany) and the appropriate software (PSt3, version 7.01; PreSens, Regensburg). The total duration of one measurement run was 48 h, since preliminary experiments showed no significant differences to metabolic rates determined over longer timescales. During the experiments, the apparent saturation was measured every 1 or 5 minutes.

The oxygen sensors were calibrated before every run in a covered beaker with streaming N_2-gas for 0% O_2-saturation and in the aerated (with the respective gas mix) closed circulation without an animal in the respiration chamber for 100% saturation. The calibration and measurements were adjusted to water temperature through a built-in temperature sensor and the given atmospheric pressure (P_{air}) at the beginning of the calibration.

For the reliable use of static respirometers to measure oxygen consumption, Steffensen (1989) points out the importance of a suitable ratio of animal- to chamber volume. All crabs used here lie in a range of 0.01 to 0.05 ($V_{ind.}/V_{chamber}$). The volume of the crabs ($V_{ind.}$) was determined by placing them in a beaker filled with seawater and measuring the volume of the displaced water. While in the beaker, the crabs were also weighed, which is necessary for subsequent calculations (see below). Later, a mean density factor $d = 0.8677$ g mL^{-1} was used to calculate the volume from the animals' weight on the basis of five direct measurements (see appendix for more details).

In the given setup, it was possible to use two respiration chambers in the same seawater basin (fig. 8). After each experimental run, the respirometers were wiped from the inside with 70%

ethanol and rinsed with deionized water to reduce contamination with aerobic microorganisms. These would otherwise interfere with the detected oxygen consumption, as heterotrophic organisms would increase the uptake of O_2 and phototrophic organisms would reduce the recorded values (Steffensen 1989). The black plastic foil as a cover may further prevent algae growth during measurements as it blocks incoming light. Depending on the size of the respirometer, the duration of the measurement and the initial bacterial load in the chamber, the water and on the animal and the animal's size, bacterial respiration is reported to possibly reach values close to 30% of the respiration rate of prawns (*Palaemonetes antennarius*, Dalla Via 1983).

Oxygen consumption of crabs ($\dot{M}O_2$) is given in nmol O_2 min^{-1} g^{-1} fresh weight. From the measured values of oxygen as percentage of air saturation, it was calculated as follows:

The absolute concentration of oxygen at 100% saturation in the respirometer was calculated from

$$c_{O_2}(100\%) = \alpha_{O_2} \cdot [(P_{air} - P_{wv}) \cdot 0.2095] \quad [3]$$

with α_{O2} as the Bunsen solubility coefficient of oxygen at a given salinity and temperature (from Boutilier et al. 1984), P_{wv} as the vapor pressure of water (from Dejours 1975) and 0.2095 representing the volume percentage of oxygen in air. Determined by the dimension of α, the concentration will be given in µM. The absolute amount of oxygen in µmol has to be related to the volume of water in the respiration chamber:

$$n_{O_2} = c_{O_2} \cdot (V_{chamber} - V_{ind.}) \quad [4]$$

With the absolute amount of oxygen at 100% air-saturation and the fresh weight of the crab (w_f), the recorded change of saturation over time ($\Delta c_{rel.}\ \Delta t^{-1}$) can be used to calculate the mass-specific oxygen consumption rate $\dot{M}O_2$ of each individual:

$$\dot{M}O_2 = n_{O_2} \cdot \frac{\Delta c_{rel.}}{\Delta t \cdot w_f \cdot 100} \quad [5]$$

The mean change of saturation over time (the mean, descending slope of the saturation) was derived in LabChart Reader (v8.0.5; ADInstruments, Oxford, UK). The values for $\dot{M}O_2$ will thus be averages for approximately 45 min – the time in which the respirometer was on closed circulation. With the selected setup, one value for $\dot{M}O_2$ is taken as a representative mean for one hour of measurement.

2.4 NMR-measurements

2.4.1 Theoretical background

Some biologically relevant isotopes (e.g. ^{1}H or ^{31}P) have a magnetic dipole moment induced by the nuclear spin. The nuclear spin of such an isotope can orientate parallel or anti-parallel to an applied magnetic field, with lower (parallel) and higher (anti-parallel) energy levels depending on its orientation. An ensemble with more spins in the energetically favorable level will produce a macroscopic, detectable magnetization. This physical process is called nuclear magnetic resonance (NMR; De Graaf 2007).

As a non-invasive and non-destructive technique, NMR spectroscopy is well suited for *in vivo* measurements, such as the determination of energy metabolism or acid-base status through ^{31}P-NMR spectroscopy. Another advantage of this technique is the simultaneous online monitoring of intra- and extracellular pH without further disturbance of the animal. This method relies on the so-called chemical shift δ, or relative resonance frequency of the signal peaks in an NMR scan (fig. 11). Different chemical shifts occur, because nuclei (even within the same molecule) absorb energy at different resonance frequencies that is heavily influenced by the magnetic fields of the surrounding atoms (De Graaf 2007). The resonance frequency of an isotope is dependent on its chemical surroundings and thus in case of inorganic phosphates also on pH. Acidic substances with a pK_a close to physiological pH are most suitable to be accurately correlated with pH, since these undergo the most rapid changes in their state of protonation. This means that changes in pH will yield greater changes in the amount of H^+ ions associated with e.g. one phosphate ion and therefore to greater changes in the chemical shift of the signal peaks of these molecules. Intracellular pH (pH_i) can easily be monitored through the analysis of the P_i peak, since free phosphates are almost exclusively concentrated in the cytosol (Moon & Richards 1973). Phosphorus compounds are ideal not only because of their pK_a value but also because their natural isotope has an odd number of nucleons and therefore has a magnetic dipole moment. For extracellular pH, a substitute phosphorus compound has to be injected, namely 3-aminopropylphosphonate (3-APP). This technique was introduced by Gillies et al. (1994) and already applied to *C. maenas* by Wermter (2009) and Kreiß (2010). These studies also report no toxic effects or metabolic processing of 3-APP and that the signal intensity remained high, even after weeks after the injection.

Through the application of position-dependent magnetic fields in addition to the static magnetic field, the spatial distribution of directed spins can be used to reconstruct an image, so-called magnetic resonance imaging (MRI; De Graaf 2007). Recent MRI techniques can be

used to study e.g. cardiovascular activity (Gatehouse et al. 2005; De Graaf 2007). *In vivo* NMR imaging techniques adopted from human medical applications might now be a way to investigate the influences of – for example – ocean acidification, hypoxia and global warming on animal cardio-physiology (Dogan 2011).

In this study, the aim is the observation of resting states, so that data on the heart rate and blood flow are comparable to standard metabolic rates. Because the animal is placed in a small chamber during the NMR measurements (fig. 9), it is crucial that this chamber is constantly supplied with aerated seawater through a flow-through system. While *C. maenas* is quite tolerant to hypoxia and minor drops in the oxygen saturation have no effect on heart rate (Taylor & Butler 1973), meaningful measurements require that the oxygen content is high and that metabolic waste products, including CO_2, do not accumulate and compromise the desired experimental conditions.

In early studies measuring the heart beat activity of crabs, metal electrodes were carefully inserted through the carapace close to the heart (e.g. Taylor & Butler 1973; 1978). They found that heart rate in *C. maenas* with a mean weight of 70 g increases with temperature, ranging from 40 bpm at 6°C to 120 bpm at 17°C. However, heart rate was also shown to depend on body size: larger animals have a lower heart rate, while increasing temperature still increases heart rate (Ahsanullah & Newell 1971). More recent studies have refrained from using invasive methods and rather measure heart rate with infra-red detectors (Wittmann 2010; Tepolt & Somero 2014).

2.4.2 Experimental setup for in vivo *NMR experiments*

All *in vivo* ^{31}P-NMR spectroscopic and MRI measurements were conducted in a 200 MHz horizontal NMR spectrometer (47/40 Biospec DBX; Bruker BioSpin GmbH, Ettlingen, Germany). Individual animals were kept in a sealed chamber of around 300 mL volume. This chamber was placed under a ^{1}H and ^{31}P tunable 50-mm-diameter surface-coil (fig. 9). The position of the coil was adjusted so that its center was above the center of the animal. Levers in

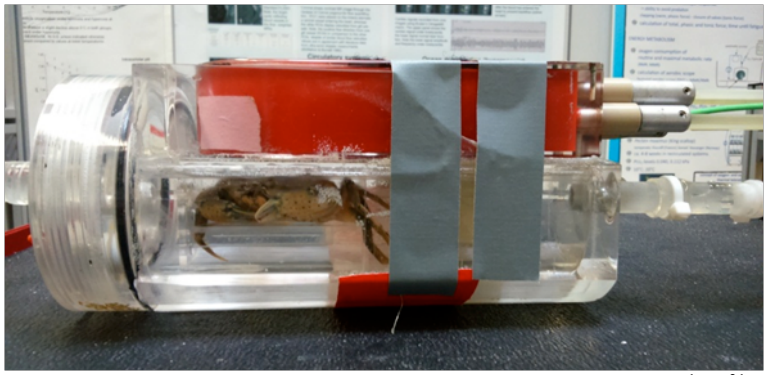

Fig. 9. Crab inside the chamber for NMR experiments. The ^{1}H, ^{31}P tunable 50 mm coil is on top. The water inlet is on the right, while the outlet is on the left.

lateral direction restricted movement of the animal and it was held directly underneath the coil by being placed on a plastic slide. The chamber was constantly supplied by a stream of seawater at the same conditions like the incubation regarding *T*, *S*, $P(CO_2)_w$ and pH_w. This setup is displayed in fig. 10.

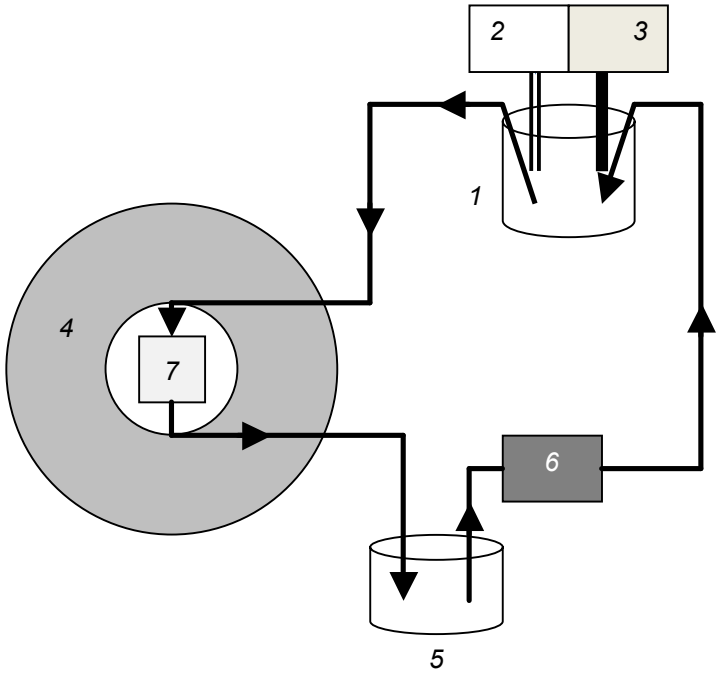

Fig. 10. Schematic design of the NMR measurement setup. 1) Water reservoir; 2) Gas-mixing pump for aeration; 3) Thermostat for temperature control; 4) Magnet of NMR-tomograph; 5) Overflow basin; 6) Peristaltic pump; 7) Holding chamber for the crab. The arrows indicate the direction of the water flow.

Before the start of the *in vivo* experiments of each individual, the animals were allowed to recover from potential handling stress to acclimate to its new setup for at least 1 h. The magnetic field homogeneity, excitation frequency and reference pulse gain were adjusted according to automatized protocols. The positions of the coil and the animal in the magnetic field were optimized with three-dimensional overview MRI scans (tripilot).

2.4.3 Simultaneous observation of intra- and extracellular pH

The intra- and extracellular pH were determined through *in vivo* ^{31}P-NMR spectroscopy, based on the pH-dependent chemical shift of two phosphorous compounds relative to phospho-L-arginine as internal standard. pH_i was derived from the chemical shift of inorganic phosphate (P_i) while a substitute compound had to be injected to determine pH_e. An unbuffered, aqueous solution of 250 mM 3-aminopropyl-phosphonate (3-APP), representing the ionic composition of the haemolymph of *C. maenas* was prepared (tab. 2; Kreiß 2010; Wittmann 2010). After the respiration experiments, the animals were weighed (see above) and injected with that solution so that a final 3-APP concentration of approximately 10 mM in the animal was reached. Therefore, it was assumed that the volume of the haemolymph is one third of the

fresh weight of the crab. In average, the injected volume was 4-5% of the respective haemolymph volume and always less than 1 mL per crab. The solution was injected through the articular membrane between the coxa and the trochanter of the third, right walking leg. No buffer was added to the solution in order to not disturb the haemolymph buffering system that had established during the incubation. Due to the acidic nature of 3-APP, the pH of the final solution was approximately 6.0. Since the injection poses physiological stress to the animals, they were given around five days in their incubation cages before being subjected to NMR experiments.

Tab. 2. Concentration of ions in haemolymph of *C. maenas* at 10°C and reduced salinity of 26.8 (after Kreiß 2010).

Ion	*c* / mM
Na^+	455.7
Cl^-	450.9
Mg^{2+}	12.8
SO_4^{2-}	11.8
K^+	11.6
Ca^{2+}	10.9

The scanning parameters for ^{31}P-spectra are summarized in tab. 3:

Tab. 3. Scanning parameters of *in vivo* ^{31}P-NMR spectra.

Parameter	Value
Measuring method	NSPECT
Repetition time	1400 ms
Number of averages	400 – 1600
Flip angle	60.0°
Attenuation	6.0 dB
Basic frequency	81.10 MHz
Receiver gain	203.00
Spectral width	83.09 ppm

In vivo ^{31}P-spectra of the whole animal were processed with Topspin 3.0 (Bruker BioSpin GmbH, Rheinstetten, Germany) as part of a software routine (CTjava, AWI, R. Wittig, personal communication): After the initial fourier transformation, phase- and baseline correction were applied to the approximate regions of the peaks of phosphor-L-arginine (PLA), P_i and 3-APP only. The endogenous signal of PLA was used as the reference for the respective chemical shifts δ (δ_{PLA} = 0 ppm; fig. 11). The peaks in the designated target ranges were picked automatically and fit to a Lorentz-distribution through a least-square method (mdcon, Bruker BioSpin, Rheinstetten). The parameters of the respective Lorentz-distributions were used to calculate the chemical shift, from which the pH-values were then calculated according to Kreiß (2010), applying the constants derived at 10°C. For P_i: pK_a = 6.79; δ_{min} = 4.24 ppm; δ_{max} = 6.59 ppm (modified after Zange et al. 1990). For 3-APP: pK_a = 7.11; δ_{min} = 24.1275 ppm; δ_{max} = 27.6275 ppm (after Gillies et al. 1994). The equations are as follows:

$$pH_e = pK_{a\ 3\text{-}APP} - \log \frac{\delta - \delta_{min}}{\delta_{max} - \delta} \quad [6]$$

$$pH_i = pK_{a\ P_i} + \log \frac{\delta - \delta_{min}}{\delta_{max} - \delta} \quad [7]$$

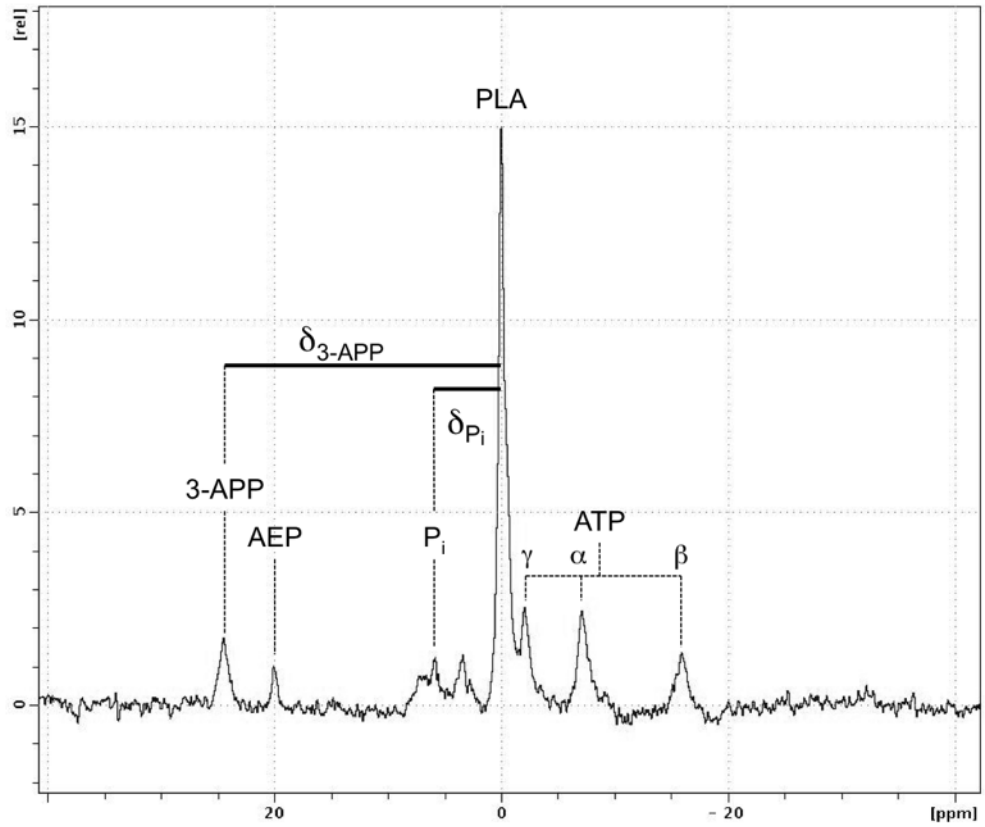

Fig. 11. *In vivo* whole-animal ^{31}P-NMR spectrum of a male *C. maenas*. The most important peaks are labeled as follows: 3-APP = 3-aminopropylphosphonate, injected to a concentration of approximately 10 mM, used to detect pH_e. AEP = 2-aminoethylphosphonat, compound that is exclusively found in male crabs (Kleps et al. 2007). P_i = inorganic phosphate, used to detect pH_i. PLA = phospho-L-arginine, used as an internal reference standard, chemical shift set to 0 ppm. ATP = adenosinetriphosphate, with α, β and γ phosphates as distinct peaks.

2.4.4 Determination of cardio-vascular performance

Cardio-vascular performance was measured through *in vivo* MRI at the incubation temperature of 8°C. After anatomical imaging based on packages of coronal (horizontal) slices from ^{1}H-RARE- and flow-map image scans, a suitable layer was selected that included a dorsal view of a cross section of the *arteria sternalis*. The rhythmic flow in this vessel was chosen as an approximate substitute of heart beat since it was not always possible to visualize the rhythmic contractions of the heart directly.

Heart rate was quantified, using the self-gated imaging software IntraGate (Bruker BioSpin GmbH, Ettlingen). From each two-minute-scan, a twenty-second-period with periodic raw signals was selected, the signal peaks were counted and heart rate in beats-per-minute (bpm) was calculated. The blood flow in cm s^{-1} was determined in phase contrasted, flow-weighed

^{1}H-image scans (FLOWMAP, fig. 12). Phase contrasted images include information about flow direction and velocity, so that the *arteria sternalis* was usually easily identified as the region with the highest directed flow in the image (Bryant et al. 1984; Gatehouse et al. 2005). Through integrated macros in the software Paravision 5.1 (Bruker BioSpin GmbH, Ettlingen), a region of interest was fitted to the artery and the included phase information was transferred into flow velocity. For the measurement parameters of the *in vivo* image scans, see tab. 4.

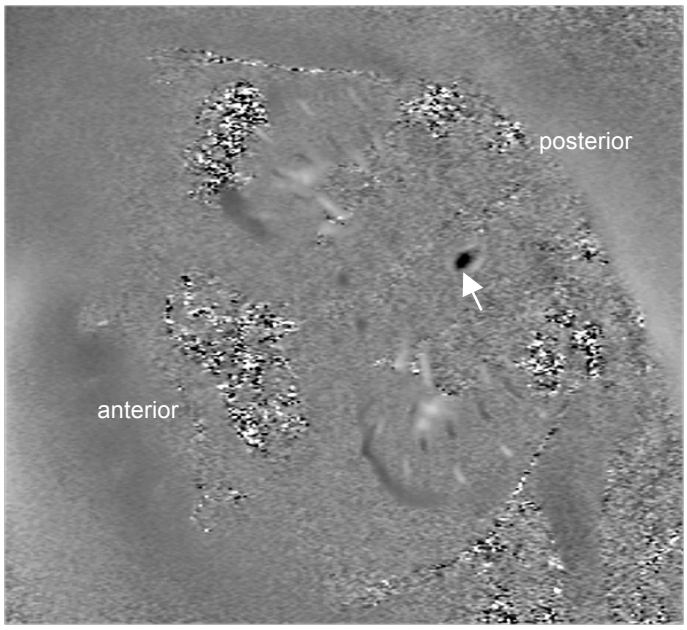

Fig. 12: Phase-contrasted (FLOWMAP) MRI scan. Coronal scan of one crab, dorsal view. Directed flow is indicated by bright or dark coloring. Dark spots indicates flow into the picture, especially pronounced in the *arteria sternalis* (white arrow). The two lateral structures next to the *arteria sternalis* are the gills.

Tab. 4. Scanning parameters of *in vivo* MR images.

Parameter	Heart rate	Flow rate
Measuring method	IntragateFLASH	FLOWMAP
Repetition time	8.00 ms	25.104 ms
Echo time	3.051 ms	12.000 ms
Number of repetitions/averages	128	16
Flip angle	45.0°	30.0°
Attenuation	13.6 dB	20.0 dB
Field of view	60 x 60 mm^2	
Matrix size	256 x 256	512 x 256
Flow encoding		slice direction
Maximum / minimum velocity		12.0 – 0.3 cm s^{-1}

2.5 Analysis of haemolymph

2.5.1 Sampling and the carbonate system of the haemolymph

The concentration of total CO_2 in the haemolymph $c(CO_2)$ was determined through gas-phase chromatography (G6890N, Agilent Technologies, Santa Clara, USA). Therefore haemolymph had to be extracted according to the following procedure: After all in vivo experiments were finished, the animals were padded dry and punctuated with an ice-cold syringe at the base of one of the walking legs, that was not previously used to inject the 3-APP solution. From the total extracted haemolymph (approximately 500 µL), two 200 µL sub-samples were taken with a gas-tight Hamilton syringe to be injected in two septum-sealed glass flasks, containing 3 mL 0.1 M HCl each. These flasks were then used for duplicate measurement of $c(CO_2)$. In case less than 500 µL of haemolymph were extracted, only one flask was filled. The remaining volume (ca. 100 µL) was transferred to 0.5 mL Eppendorf tubes and stored at -20°C until further processing for the ion chromatography (see below).

For gas-phase chromatography, calibration standards were established by dilutions of a CO_2-solution (1 g CO_2/L, Reagecon, Shannon, Ireland) and measured in duplicates of the following concentrations in mM: 5.681, 11.361, 22.723 and 33.585 (see fig. A2 in the appendix). Blanks, accounting for the residue CO_2 in air and HCl were measured in duplicate with the addition of 200 mL milliQ water. The area of the respective peak was taken as the measure for the CO_2-concentration of the sample. From $c(CO_2)$ and pH_e it was possible to calculate $P(CO_2)_e$ and $[HCO_3^-]_e$ according to Heisler (1986) and Pörtner et al. (1990) with CO_2 solubility coefficient α and apparent first dissociation constant pK_a''' calculated after Heisler (1986, see appendix for an example):

$$P(CO_2)_e = \frac{c(CO_2)}{10^{pH_e - pK_a'''} \cdot \alpha + \alpha} \quad [8]$$

$$[HCO_3^-]_e = P(CO_2)_e \cdot \alpha \cdot 10^{pH_e - pK_a'''} \quad [9]$$

2.5.2 Inorganic ion concentration

In the remaining volume of the haemolymph-samples, the concentrations of Na^+, K^+, Mg^{2+}, Ca^{2+} and Cl^- were determined through ion chromatography (ICS1500 for cations and ICS2000 for anions, Dionex, Sunnyvale, USA). The area of the signal peak was taken as a measure for ion concentration. To reduce background conductivity, a conductivity cell and a self-regenerating suppressor at 32 mA were used. Cations were separated on an IonPac CS16 (Dionex, Sunnyvale) column with 30 mM methane-sulphonic acid as an eluent. An IonPac CG16

column was used as a guard to pre-filter the sample solution and to avoid an overloading of the actual analytical column. The flow rate was 0.36 mL min^{-1} at a temperature of 40°C. As a reference, the signal areas of dilutions of ion standards (Combined Six Cation Standard-II, Dionex, Sunnyvale) were used to quantify the concentration in mM (see fig. A3 in the appendix). Haemolymph samples were measured in a 1:300 dilution with milliQ water. Aside from the absolute concentrations, the concentrations of K^+, Mg^{2+} and Ca^{2+} were also normalized to the concentration of Na^+, to differentiate between a general increase in total cation concentration and a fractional increase of the single ions.

Anions were measured in a 1:2100 dissolution, derived from the previously established dissolutions used to measure the cations. The reference standard was Dionex Combined Five Anion Standard (Dionex, Sunnyvale, see fig. A4 in the appendix). Anions were separated on a AS11-HC analytical column, with an IonPac AG-11 as guard column. The suppressor current intensity for anions was 23 mA. As eluent, 30 mM KOH at a flow rate of 0.30 mL min^{-1} was used. The column and cell temperature was 30°C.

2.6 Statistics and data analysis

From the continuous recordings of $\dot{M}O_2$, the 15%-percentiles were derived. The mean of the lowest 15% of values were assumed to represent the SMR, while the mean of the highest 15% was defined as RMR. This way, biological variability and measurement errors are accounted for (Dupont-Prinet et al. 2010). Especially RMR is defined as "unrestricted activity" and accordingly the values vary over time. Outliers are those values smaller (for SMR) or larger (for RMR) than the mean of the 15%-percentiles ± two-times the standard deviation. From the mean SMR and RMR of each animal, the absolute and factorial routine aerobic scope were calculated:

$$\text{Absolute routine aerobic scope} = \text{mean RMR} - \text{mean SMR} \quad [10]$$

$$\text{Factorial routine aerobic scope} = \frac{\text{mean RMR}}{\text{mean SMR}} \quad [11]$$

The first hour of measurement was not considered in the calculation of SMR and RMR, because it seems to reflect forced activity by handling stress from the transfer of the animal in the respiration chamber. Values for pH_i and pH_e are given as means from at least ten consecutively acquired ^{31}P-NMR-spectra per animal (maximum of 50 spectra), excluding at least the first hour of measurement after the animals were placed in the magnet.

All data per incubation group were checked for normal distribution through the Shapiro-Wilk-test and tested for equal variance. Outliers were identified through Grubb's test at $\alpha = 0.05$. To identify statistically significant differences between groups, the values for the respective parameters were compared with each other, using ANOVA at $\alpha = 0.05$ with Student-Newman-Keuls post-hoc test. In case no normal distribution or no equal variance was found within the data set, significant differences were tested through non-parametric tests (Kruskal-Wallis ANOVA on ranks with Dunn's post-hoc test). If not stated otherwise, all results are given as group mean ± standard deviation. All statistical analyses were conducted with SigmaPlot 12.0 (Systat Software, 2010).

3. Results

3.1 Incubation and water parameters

The mean water parameters of all groups are summarized in tab. 5. For the weekly changes, see fig. A1 in the appendix. No large variations in $P(CO_2)_w$ and pH_w were found, and with the exception of the first two weeks in the control group, T_w was kept fairly constant. Salinity declined progressively in all groups from 34.5 to a bout 32.0 at the end of the experiments. A depression of pH_w from 8.13 to 8.02 and $[HCO_3^-]_w$ from 2.2 to 1.6 mM was found in the control group at the 8th week of incubation, but this is was two weeks after the NMR experiments and 4 weeks before the haemolymph sampling. Mortality occurred in all groups, with one dead animal in each normocapnic and two dead in the hypercapnic groups. All surviving animals used for the analysis were male, thus excluding the one female in group 3.

Tab. 5. Water parameters of the incubation. Group size describes the number of animals used for the final data analysis. One surviving female in group 3 was taken out of the subsequent data analysis. Values are group means ± standard deviation of the weekly measurements of the parameters.

Group	Group size / *n*	*T*w / °C	*S* / PSU	$P(CO_2)_w$ / ppm	$[HCO_3^-]_w$ / mM	pH_w
control	7	8.24 ± 0.47	32.84 ± 0.93	440 ± 37	2.21 ± 0.25	8.12 ± 0.04
1	5	8.46 ± 0.09	32.76 ± 1.16	1820 ± 64	2.24 ± 0.14	7.50 ± 0.03
2	6	8.27 ± 0.13	32.60 ± 1.04	390 ± 55	1.08 ± 0.16	7.85 ± 0.05
3	4 + 1 ♀	8.24 ± 0.12	32.84 ± 1.05	1820 ± 53	1.10 ± 0.18	7.19 ± 0.07

3.2 Metabolic rates

Continuous recordings of the oxygen consumption for 48 h usually showed a pattern, where phases of relatively low values were interrupted by periods of spontaneous activity, exemplified for animal “K9” (control conditions) in fig. 13. From the initially high oxygen consumption rates at the beginning of the measurement, the values gradually declined, so that the phases of lowest oxygen consumption were usually more frequent towards the end.

The mean SMR and RMR for each group are shown in fig. 14. No significant deviations were found from a mean SMR of 10.55 ± 0.89 nmol min^{-1} g^{-1} in the control group. The SMR in group 1 of 13.24 ± 3.23 nmol min^{-1} g^{-1} under hypercapnic conditions was significantly higher than the SMR under conditions of reduced bicarbonate in groups 2 and 3, with rates of 8.68 ± 2.97 and 9.17 ± 2.53 nmol min^{-1} g^{-1}, respectively. The absolute differences are more pronounced in the RMR, where hypercapnic conditions alone lead to a significantly increased RMR of 48.62 ± 7.05 nmol min^{-1} g^{-1}, compared to 27.66 ± 5.06 nmol min^{-1} $g^{-}1$ at hypercapnia

and reduced $[HCO_3^-]_w$ (group 3). The RMR of group 3 was the lowest among all treatments, even being significantly lower than the control values at 40.67 ± 5.79 nmol min^{-1} g^{-1}.

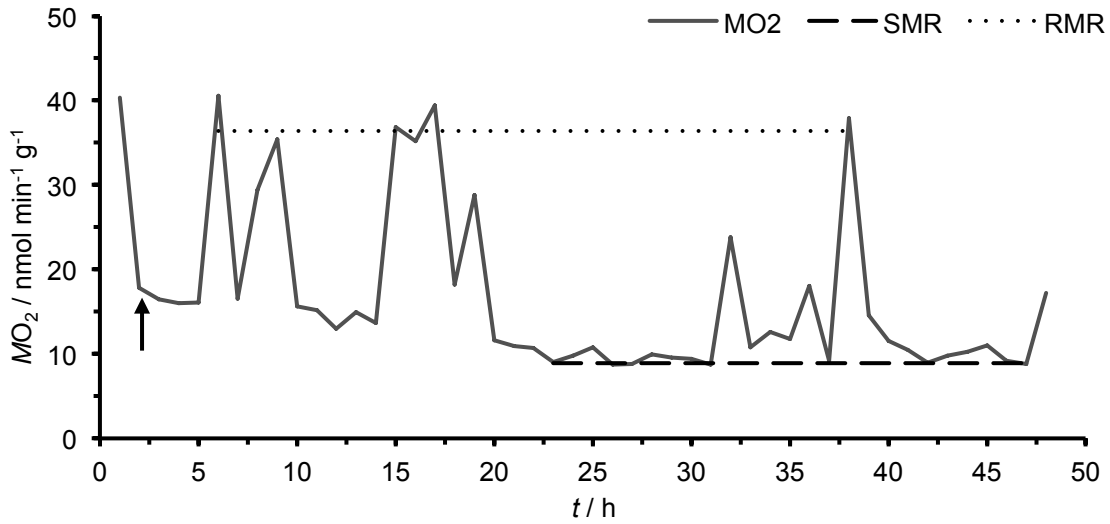

Fig. 13. Typical example for a time series of recorded metabolic rates. $\dot{M}O_2$ was calculated from the decline in oxygen saturation measured during 45 min of closed circulation in an intermittent flow respirometer at 8°C. Each data point represents the mean decline of saturation for one hour. Data derived from animal "K9" under control conditions. Dashed line = mean SMR, representing mean of lowest 15%; dotted line = mean RMR, representing mean of highest 15% of all data points, excluding the first hour. The arrow thus marks the beginning of the analysis

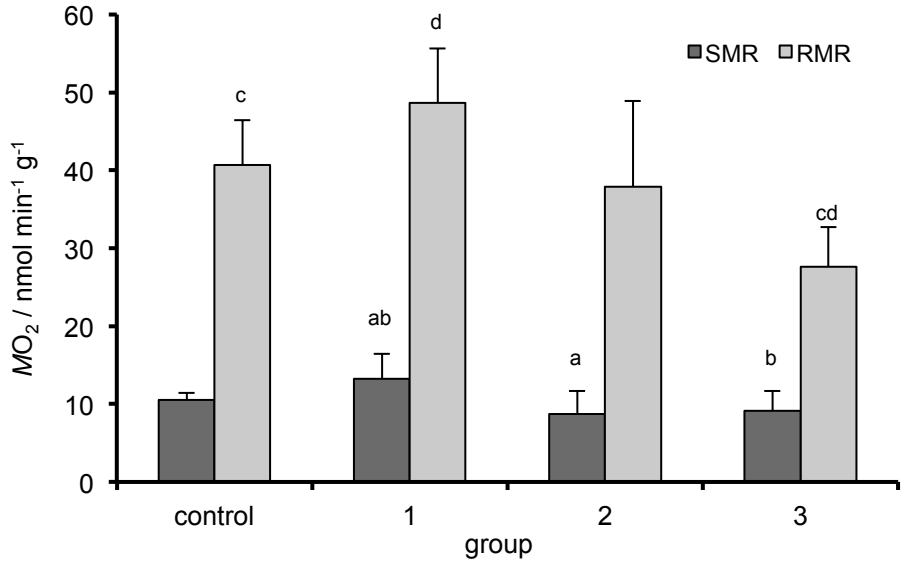

Fig. 14. Standard and routine metabolic rate. Values were calculated for each individual from the highest and lowest 15% from 48 h of continuous recordings of $\dot{M}O_2$, excluding the first hour. Group 1: Hypercapnia; group 2: reduced $[HCO_3^-]_w$; group 3: Hypercapnia & reduced $[HCO_3^-]_w$. T_w = 8°C. Identical letters indicate significant differences (ANOVA, $P < 0.05$).

Accordingly, group 3 shows the smallest absolute routine aerobic scope (difference between RMR and SMR, fig. 15A), being significantly reduced compared to all other groups. Regarding the proportional changes of RMR and SMR (factorial routine aerobic scope: RMR/SMR), no changes were found across the experimental groups, with values pending around 3.5 (fig. 15B).

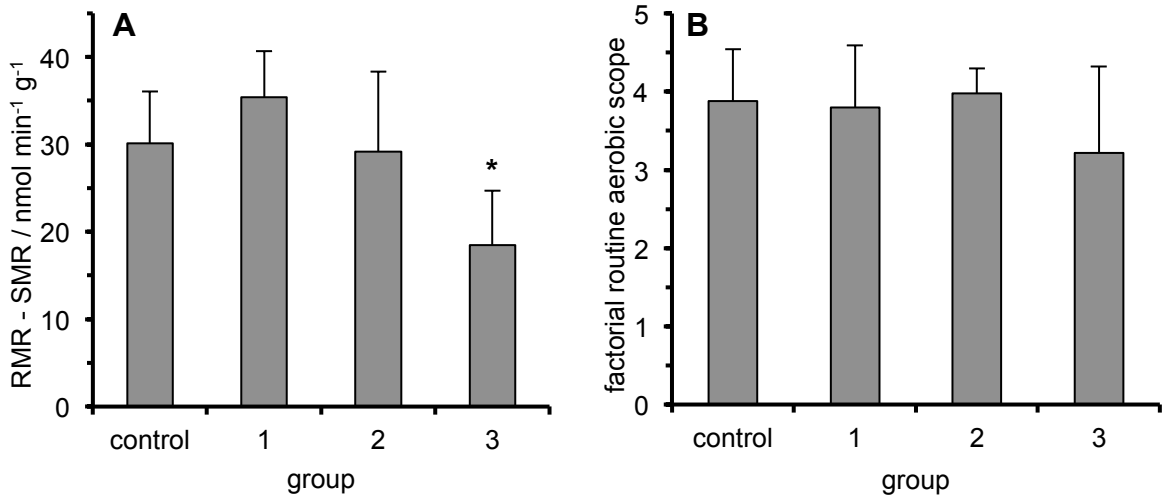

Fig. 15. Absolute and factorial routine aerobic scope. Group 1: Hypercapnia; group 2: reduced $[HCO_3^-]_w$; group 3: Hypercapnia & reduced $[HCO_3^-]_w$. T_w = 8°C. **A)** Absolute routine aerobic scope, calculated from subtracting the individual SMR from the individual RMR. **B)** Factorial routine aerobic scope (RMR / SMR), calculated from averaging the individual ratios. The asterisk indicates significant difference to the other groups (ANOVA, $P < 0.05$).

3.3 Cardiac performance

Blood flow and heart rate were determined from ^1H *in vivo* IntraGateFLASH MRI scans of a cross section of the *arteria sternalis* (fig. 16). While heart rate was found to be constant at about 48 bpm (fig. 17A), blood flow in group 1 was significantly higher, compared to groups 2 and 3 (fig. 17B). It decreased by almost 1 cm s^{-1} from 3.42 ± 0.20 cm s^{-1} under hypercapnia to 2.45 ± 0.49 cm s^{-1} when $[HCO_3^-]_w$ was artificially reduced in combination with elevated $P(CO_2)_w$ (group 3). The patterns of the changes in flow rate resemble those of the changes in RMR, meaning that group 1 has the highest and group 3 the lowest values.

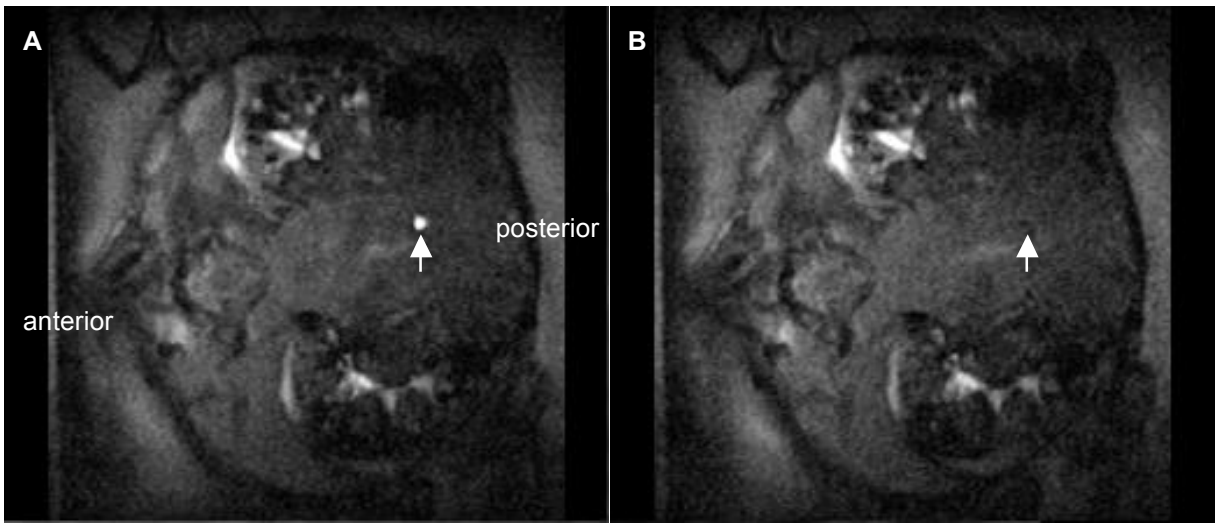

Fig. 16. IntraGateFLASH MRI-scans of the heart beat, visualized in the *arteria sternalis*. A) Systolic phase; **B)** Diastolic phase. The arrow marks the position of the sternal artery, marked by high blood flow during the systolic phase. The gills (lateral) are also easily identified by high liquid flow.

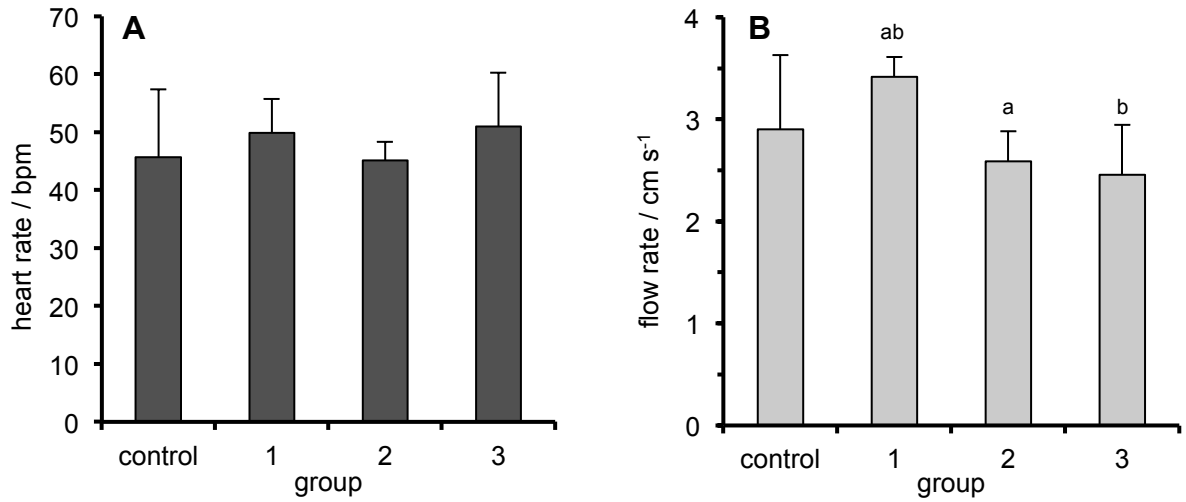

Fig. 17. Heart rate (A) and haemolymph flow rate (B). Both values were determined through ^{1}H *in vivo* NMR image scans at a plane, visualizing the *arteria sertnalis*. Group 1: Hypercapnia; group 2: reduced $[HCO_3^-]_w$; group 3: Hypercapnia & reduced $[HCO_3^-]_w$. T_w = 8°C. Identical letters indicate significant differences (ANOVA, $P < 0.05$).

3.4 Haemolymph acid-base parameters

Values of pH_i and pH_e in the individual animals remained more or less constant over time (fig. 18) and no significant changes in the mean intra- or extracellular pH were found in all groups (fig. 19). pH_i was determined to be close to 7.20 ± 0.08 throughout, while pH_e ranged from 7.86 ± 0.06 in the control group to 7.79 ± 0.09 in group 3.

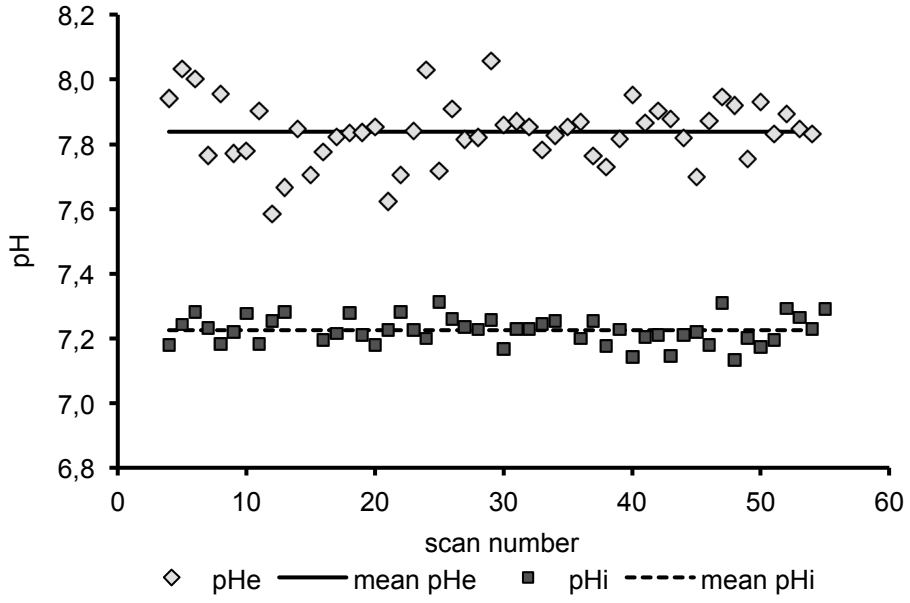

Fig. 18. Time course of intracellular (pH_i) and extracellular (pH_e) pH. Each data point is derived from one ^{31}P NMR spectrum without special localization of the signal, thus being representative for the whole-animal average haemolymph and tissue pH. For every value in pH_e, there usually is a respective pH_i, unless one of the peaks could not be clearly detected. One scan lasted about 10 – 20 min, interrupted by prolonged breaks between two scans where MRI scans were done. Animal "2.5". pH_i = 7.22 ± 0.04; pH_e = 7.84 ± 0.10.

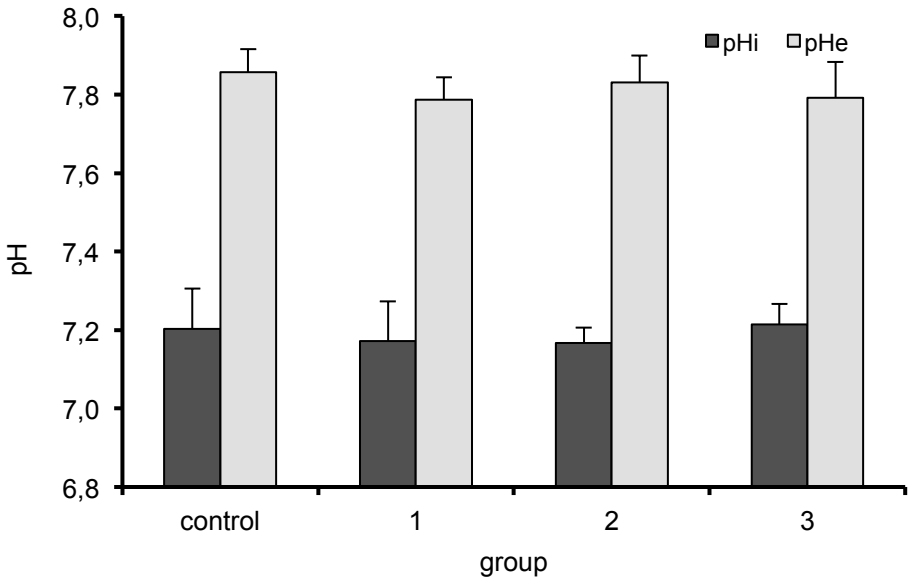

Fig. 19. Intracellular (pH_i) and extracellular (pH_e) pH. The data are derived from whole-animal *in vivo* ^{31}P NMR spectra without special localization of the signal. The respective pH values are thus representative for whole-animal average haemolymph and tissue pH. Group 1: Hypercapnia; group 2: reduced $[HCO_3^-]_w$; group 3: Hypercapnia & reduced $[HCO_3^-]_w$. T_w = 8°C.

From the measurement of total $c(CO_2)$ in the haemolymph and pH_e, haemolymph $P(CO_2)$ and $[HCO_3^-]_e$ can be calculated. An increase of $c(CO_2)_e$ in groups 1 and 3 at constant pH_e paralleled significantly increased $P(CO_2)_e$ and $[HCO_3^-]_e$ in the crabs incubated at elevated $P(CO_2)_w$, when compared to the normocapnic groups (fig. 20). A $P(CO_2)_e$ of 2.84 ± 0.78 torr was found as mean control value, which did not differ significantly from the 2.80 ± 0.74 torr in group 2. $P(CO_2)_e$ nearly doubled under hypercapnic incubation conditions to values of 5.21 ± 1.61 torr in group 1 and 4.85 ± 1.70 torr in group 3. This pattern in the mean values is similarly found for $[HCO_3^-]_e$: Reductions in seawater bicarbonate only correspond to minor, insignificant depressions in the respective haemolymph concentration under either hyper- or normocapnic incubation. If $[HCO_3^-]_e$ is plotted against pH_e and $P(CO_2)_e$ (also known as "Davenport diagram"), it becomes evident that the values for groups 1 and 3 are elevated above the non-bicarbonate buffer line (fig. 21).

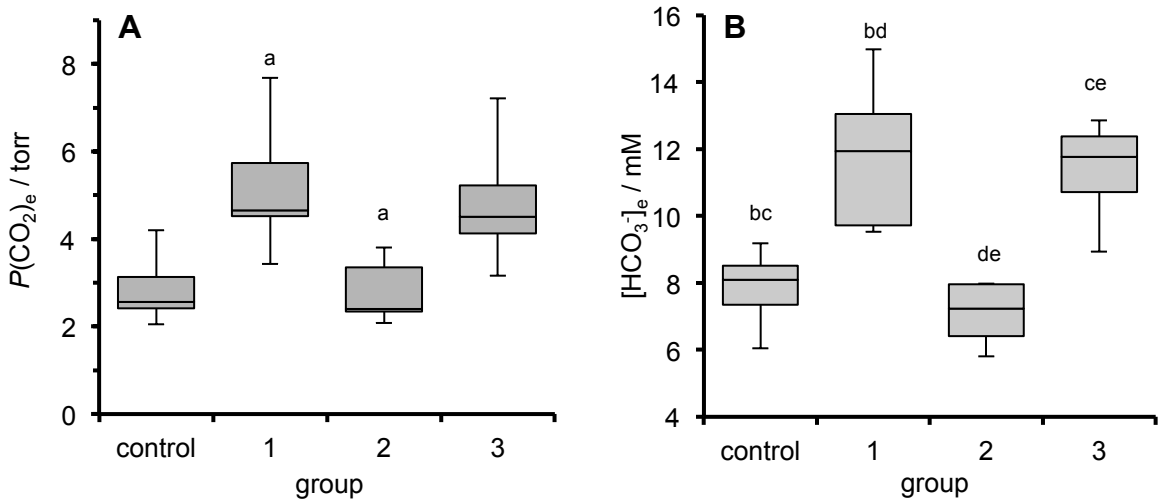

Fig. 20. Haemolymph CO_2 parameters. A) Haemolymph $P(CO_2)$. **B)** Haemolymph $[HCO_3^-]$. Boxplots show group minimum, 1st quartile, median, 3rd quartile and group maximum (from bottom to top). Group 1: Hypercapnia; group 2: reduced $[HCO_3^-]_w$; group 3: Hypercapnia & reduced $[HCO_3^-]_w$. T_w = 8°C. Similar letters indicate significant differences (ANOVA, $P < 0.05$).

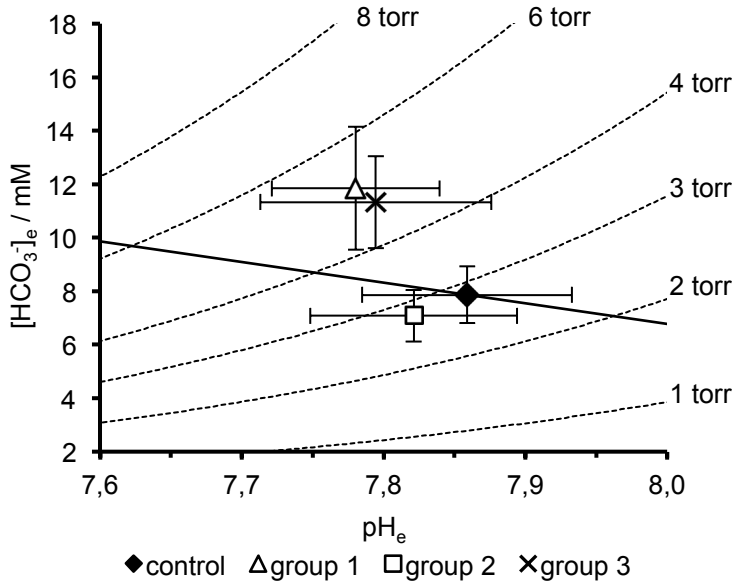

Fig. 21. pH / bicarbonate diagram for the haemolymph of *C. maenas*. Values are group means ± standard deviation. Dashed lines are representing isopleths for $P(CO_2)_e$. The solid, straight line represents the non-bicarbonate buffer value in the haemolymph, with the slope calculated as $\Delta[HCO_3^-]_e/\Delta pH_e$ = -7.7158, after Truchot (1976a) with protein concentration = 50 g/L after Truchot (1973). Group 1: Hypercapnia; group 2: reduced $[HCO_3^-]_w$; group 3: Hypercapnia & reduced $[HCO_3^-]_w$. T_w = 8°C.

3.5 Ion composition of the haemolymph

An increase of cations over control levels has been found in all experimental groups, with the highest cation concentrations found under hypercapnic conditions, combined with reduced seawater bicarbonate (group 3; tab. 6). This increase is mainly reflected in elevated $[Na^+]$ and $[Mg^{2+}]$, compared to control conditions. Even though $[Ca^{2+}]$ was significantly increased in groups 1 and 3 over the concentrations in group 2 and the control, the absolute changes are

quite low, compared to the changes in $[Na^+]$ and $[Mg^{2+}]$. The largest increase of $[Ca^{2+}]$ was found from 11.3 ± 1.3 mM under control conditions to 13.21 ± 0.94 mM in group 3. $[Mg^{2+}]$ increased much more significantly between these two groups: While concentrations of 21.6 ± 3.0 mM were found in the control group, 32.0 ± 1.7 mM were measured in group 3. However for Mg^{2+}, no significant differences could be identified between experimental conditions. $[K^+]$ seems to remain constant at average levels of around 13 mM in all groups.

Tab. 6. Concentrations of single ions in the haemolymph. Concentrations are given in mM. Total concentrations are the sum of means of the single ions in each group. Group 1: Hypercapnia; group 2: reduced $[HCO_3^-]_w$; group 3: Hypercapnia & reduced $[HCO_3^-]_w$. T_w = 8°C. The number of asterisks indicate significant differences to the control group at various levels of significance (ANOVA, $P < 0.05$ = *, $P < 0.01$ = **, $P < 0.001$ = ***). The increase of calcium in groups 1 and 3 is also significant to group 2. The decrease of chloride in group 2 is also significant, compared to group 3.

Ion	Control	Group 1	Group 2	Group 3
Na^+	497 ± 33	533 ± 18 *	525.7 ± 8.9	540 ± 16 *
K^+	12.7 ± 1.6	14.0 ± 1.4	15.0 ± 2.3	12.4 ± 1.0
Mg^{2+}	21.6 ± 3.0	29.3 ± 4.8 **	27.5 ± 3.3 **	32.0 ± 1.7 ***
Ca^{2+}	11.3 ± 1.3	12.93 ± 0.48 *	12.25 ± 0.65	13.21 ± 0.94 *
Total cations	543 ± 39	589 ± 25	580 ± 15	597 ± 20
Cl^-	452 ± 19	445 ± 28	416 ± 20 *	473 ± 22
HCO_3^-	7.9 ± 1.1	11.8 ± 2.3 ***	7.08 ± 0.96	10.2 ± 3.0 **
Total ions	1003 ± 59	1046 ± 55	1003 ± 36	1080 ± 45

Looking at the concentrations of K^+, Mg^{2+} and Ca^{2+} in relation to Na^+, the changes in $[Mg^{2+}]$ become even more pronounced (fig. 22). While in the control group, the concentration of Mg^{2+} relative to $[Na^+]$ is 4.4%, it significantly increases to almost 6% in group 3. This elevated ratio is less for the other experimental groups, but the increases are still significant. The ratios of $[K^+]$ and $[Ca^{2+}]$ to $[Na^+]$ are constant, with averages around 2.5%.

The concentrations of Cl^- are showing a different pattern compared to $[Na^+]$, with the lowest values determined in group 2 at reduced $[HCO_3^-]_w$ (tab. 5, fig. 23). With just 416 ± 20 mM, this concentration was significantly lower than in the control group (452 ± 19 mM) and in group 3 (473 ± 22 mM). Group 3 also showed the highest concentration of Cl^- and the highest total ion concentration of 1080 ± 45 mM. It is striking that the concentration of chloride is in some cases substantially lower than the concentration of sodium alone. The largest gap between the two major ions is found in group 2, where $[Cl^-]$ is about 110 mM less than $[Na^+]$, a trend that is also reflected in the concentration changes relative to control conditions (fig. 23). Here too, only the relative change of $[Cl^-]$ in group 2 is significantly different, with a depression of about 8%, relative to control values. Hypercapnic conditions in group 1 did not affect

[Cl^-] in the way it affected [Na^+]: While [Na^+] significantly increased both in absolute and relative values compared to control conditions, [Cl^-] remained at control levels. Only under hypercapnia and reduced $[HCO_3^-]_w$ (group 3) did both concentrations increase, while the absolute and relative increase in [Cl^-] was not significant.

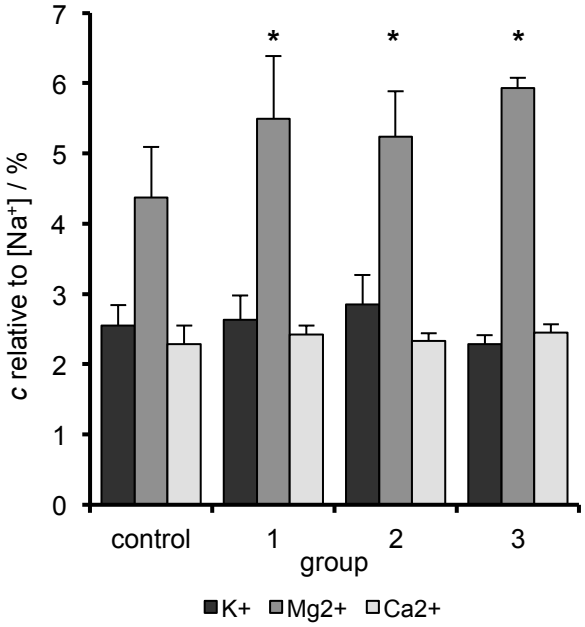

Fig. 22. Concentrations of K^+, Mg^{2+} and Ca^{2+}, relative to [Na^+]. Values are group means of the individual ratios in each animal + standard deviation. Group 1: Hypercapnia; group 2: reduced $[HCO_3^-]_w$; group 3: Hypercapnia & reduced $[HCO_3^-]_w$. T_w = 8°C. Asterisks indicate significant changes compared to control conditions (ANOVA, $P < 0.05$).

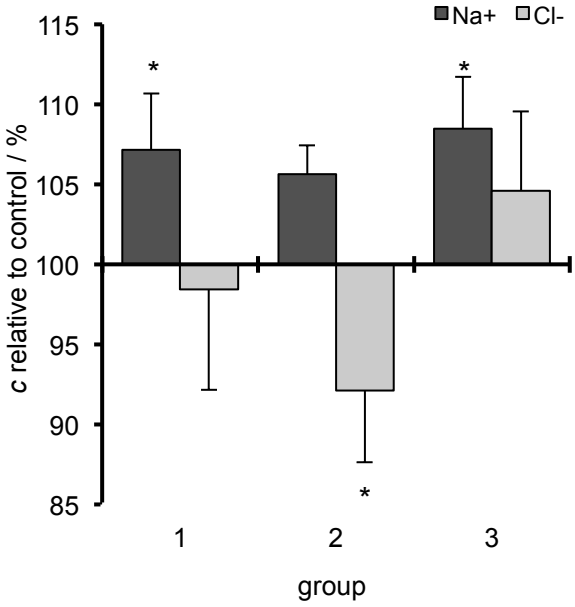

Fig. 23. Concentrations of Na^+ and Cl^-, relative to control. Vales are means + standard deviation of individual absolute values normalized to the control group mean. Group 1: Hypercapnia; group 2: reduced $[HCO_3^-]_w$; group 3: Hypercapnia & reduced $[HCO_3^-]_w$. T_w = 8°C. Asterisks show significant differences from the control group (ANOVA, $P < 0.05$).

The total concentrations of the measured ions are slightly above 1 M and do not differ greatly between the groups. Slightly higher average concentrations were measured in the two hypercapnic incubation groups 1 and 3, compared to the two normocapnic incubations (tab. 6).

4. Discussion

Individuals of the shore crab *Carcinus maenas* have been exposed to various acidic seawaters. Hypercapnia alone does not seem to affect metabolic rates and cardiac activity while pH_e is regulated to control values, most likely by an uptake of bicarbonate from the seawater. A reduced availability of bicarbonate from that source also does not affect acid-base and ion regulation differently, but it leads to depressions in metabolic rates and blood flow, compared to hypercapnic incubation alone. This suggests a so far unknown pathway how seawater carbonate alkalinity is detected and how it can affect the animal's metabolism directly.

4.1 Method and error discussion

4.1.1 Incubation and water parameters

Constant values of pH_w, $P(CO_2)_w$ and $[HCO_3^-]_w$ over the time of incubation should have led to successful adaptation of the shore crab *C. maenas* to the respective conditions. Mortalities were low and nearly even across all groups and could mostly be attributed to already existing fractures of the shell. The slightly lower T_w in the first two weeks of incubation of the control group were due to a lower ambient air-temperature at that time which was adjusted before the start of the other incubation groups. A steady decline in salinity might be attributed to the spring season with higher input of freshwater through rain, which also affected this incubation, since the seawater was brought to the institute by ship from the North Sea. The drop of pH_w and $[HCO_3^-]_w$ in the control group in week 8 was only transient and at least two weeks in between two experimental steps. A large influence on the presented results thus seems unlikely. The ambient temperature was intentionally kept close to the average natural conditions in the North Sea (Tepolt & Somero 2014) to validly quantify the SMR as a representative for the minimum sustainable energy demand of the shore crab (Fry 1971).

4.1.2 Respirometry

Oxygen uptake determined in intermittent flow respirometers at 8°C yielded SMRs of around 12 nmol min^{-1} g^{-1} under control conditions, which is in line with reports for fasting animals at similar weight and temperature (Robertson et al. 2002). It is shown again, that an intermittent flow design and the use of fiber-optic oxygen sensors for continuous recordings seem ideal to quantify SMR: Earlier studies using closed (e.g. Wallace 1972) or flow-through respirometers (Klein Breteler 1975; Taylor & Wheatly 1979) usually report values of 25 nmol min^{-1} g^{-1} for a crab with w_f = 25 g at T = 10°C (Wallace 1972; Taylor & Butler 1978). To put it into relation,

this is almost twice as high as the SMR for crabs at the same weight under control conditions in this study. By taking the average of the highest 15% of continuously recorded values of $\dot{M}O_2$ to calculate RMR, even the frequency of active phases during the measurement will affect the final values: If under the given conditions, the crab is more active (e.g. through spontaneous movement), leading to a higher frequency of high peaks in $\dot{M}O_2$, the average values of RMR will also be higher, compared to a crab which remains quite calm.

4.1.3 In vivo *MRI*

Two-dimensional MRI-scans of a layer between -11.00 and -13.00 mm off the magnetic center at a slice thickness of 1.90 mm proved to yield the best images and cardiac signals among all animals. At least three values from different scans for heart rate and flow rate were determined for each animal, evenly distributed over the duration of the NMR-experiments.

The non-invasive detection of heart rate via self-gated IntraGateFLASH MRI in a slice through the *arteria sternalis* led to mean values of 40 – 50 bpm under all conditions. Using animals similar in size and measured at the same temperature as in this study, Wittmann (2010) reported similar heart rates determined with laser-doppler sensors glued to the carapace. This indicates the validity of the applied MRI techniques, initially developed for mammals. It has to be noted that due to the setup for the NMR experiments in this study no continuous recordings of the heart rates for prolonged time were possible. This prevents any conclusion, whether the applied incubation conditions should have an effect on e.g. the duration or the frequency of the depressions in heart beat of *C. maenas* (Cumberlidge & Uglow 1977). Scans without a clear cardiac signal have been recorded, but may be caused by subtle movements of the crab. To reduce the signal-to-noise ratio, a compromise was made between spatial and temporal resolution of the NMR measurements (Dogan 2011): The selected matrix sizes allowed for the detection of sufficiently fine changes in haemolymph flow and clearly identifiable heart rates at a reasonable scanning time of less than three minutes per MRI scan.

The non-invasive measurement considerably facilitated the analysis. The handling stress for the crabs could be presumed to be minimal, as they were only fixed to remain stationary. In phase-contrasted FLOWMAP MRI, the *arteria sternalis* was easily identified as the largest vessel with the highest directed flow (fig. 12). The region of interest could thus be defined, to allow for accurate measurements of the blood flow rate. For *C. maenas*, this is the first study to determine blood flow in the *arteria sternalis*. The values measured through phase-contrasted MRI scans should be compared to values derived from heated thermo-coupled

probes, inserted into the respective blood vessels of lobsters *Panulirus interruptus* (Belman 1975) and to those from Dogan (2011) for *Cancer pagurus*, measured the same way as in this study: The two larger crustaceans had a higher blood flow (e.g. 7 cm s^{-1} in *C. pagurus*, compared to 3 cm s^{-1} in this study), which is attributed to the larger diameter of their arteries (Eckert et al. 2002; Dogan 2011). The determination of blood flow through phase-contrasted MRI thus seems to be of reasonable quality to investigate changes in cardio-vascular activity even of smaller crustaceans.

4.1.4 Measurements of the haemolymph acid-base status and ion composition

Even though ^{31}P-NMR spectra were processed automatically, the phase correction, which determines the position of the peaks in the spectrum and the detection of the peaks of P_i and 3-APP was not always correct. This was most likely due to problems with the shim (i.e. the homogeneity of the magnetic field) that was only possible to be adjusted to ^{1}H and not to ^{31}P resonance frequencies. The respective chemical shift had thus to be determined manually for a small fraction of the spectra. Considering that only whole animal scans were recorded, no distinction between single tissues could be made. In theory, the biggest tissue or the one containing the highest amount of P_i will dominate the position of the respective peak in the spectrum. Changes in individual tissues should be assessed through high-precision direct measurements, so far limited to extraction techniques (e.g. Pörtner et al. 1990). Wermeter (2012) tried to establish suitable, localized NMR techniques for the determination of pH in crabs, but the available equipment did not allow for accurate measurements within a reasonable scanning time. A similar problem with the localization of the signal exists for pH_e. Many authors report the extraction of prebranchial haemolymph to measure pH_e. The differences in post- and prebranchial pH_e are supposed to be small – below 0.03 units within one crab at a given temperature (Truchot 1973) – so measurements at whole-animal level should still be valid, since this variation is beyond the resolution of pH measurements through ^{31}P-NMR spectroscopy.

Values of pH_e around 7.8 in all groups are in good agreement with various literature studies (e.g. Truchot 1973; 1981; 1984; Appelhans et al. 2012), which indicates that the constants used to calculate pH_e from the chemical shift of the 3-APP signal in ^{31}P-NMR spectra are reasonable. This also applies to the determination of pH_i, since mean pH_i was up to 0.6 units lower than pH_e, in line with literature data (Henry & Wheatly 1992).

The quality of the values for $P(CO_2)_e$ and $[HCO_3^-]_e$, as well as for haemolymph ion concentrations is only as good as the extraction of the haemolymph. Especially in small individuals,

inserting the needle without rupturing the gill chamber (then extracting seawater rather than haemolymph) or the leg muscles (possible contamination with cytosolic compounds) is quite difficult. To reduce contamination of the sample by seawater remaining on the crab's surface, animals were padded dry, before inserting the needle. The whole process has to be done quickly, in order to keep the stress response of the animal to a minimum. Otherwise, exposure to air and invasive handling might result in disturbances, especially of the acid-base status, possibly influenced by the onset of anaerobic metabolism. However, the haemolymph $P(CO_2)$ and $[HCO_3^-]$ under control conditions were comparable to the results obtained by Truchot (1973; 1981; 1984).

Concerning the relationship between $[HCO_3^-]_e$, pH_e and $P(CO_2)_e$ (fig. 21), it has to be mentioned that the non-bicarbonate buffer line was not determined experimentally, but calculated with an assumed, fixed protein concentration (Truchot 1973; 1976a). Oxygen capacity and protein concentration both linearly correlate with the non-bicarbonate buffering value, indicating a key role of haemocyanin – the main protein in the haemolymph – in non-bicarbonate buffering (Truchot 1976a). The haemolymph protein concentration of 50 g/L used to calculate the slope of the buffer line was deliberately chosen to be higher than the average concentration of around 40 g/L, but then again not out of the ordinary for crabs at this temperature (Truchot 1973). This way, the qualitative interpretation of the pH/bicarbonate diagram (fig. 21) is still valid, even without the measurement of changes of non-bicarbonate buffer values, which may change for example due to the increase in the concentration of free amino acids in the haemolymph (Hammer et al. 2012).

The concentration of inorganic ions in the haemolymph of *C. maenas* depends heavily on their concentrations in the external medium. Any control values as well as the observed increases in all experimental groups have to be related to the measured decline in salinity from initially 34.5 to 32.0 at the point of sampling (fig. A1B in the appendix). Values determined in this study are roughly in line with literature findings (e.g. Truchot 1975; 1976b; 1979; Wittmann 2010). While ion chromatography generally is an accurate quantification technique, the samples have to be highly diluted (here 1:300 for cations and 1:2100 for anions from the same subsample), so personal handling might have affected the absolute values. Relative changes within cations or anions should still be comparable and will thus allow for an analysis (fig. 22 & 23). Multiple measurements on one sample were conducted if the general concentrations deviated too much from the estimated (literature) values, in order to eliminate mistakes possibly introduced by the dilution step. All samples were randomly measured and the system was frequently flushed with milliQ water to avoid an ion overload on the separator columns. The

ion concentrations, especially of the cations, deviate from the assumed concentrations that were used to prepare the 3-APP carrier solution (tab. 2; tab. 6). But given the facts that the injected volume was less than 1 mL and the crabs were kept at ambient salinity for at least two more weeks before the sampling of the haemolymph, any disturbances should have been well compensated for. Last not least, the injection did not lead to increased mortality. Respiration rates in the control group were similar before and after the injections (tab. A3 in the appendix).

4.2 Efficiency of acid-base regulation and the role of ion exchange processes

Comparable to other efficient iono- and thus acid-base regulating crustaceans, *C. maenas* was able to compensate for changes in pH_i and pH_e after four weeks of exposure to hypercapnia through an active increase of bicarbonate in its haemolymph (fig. 21; Pane & Barry 2007; Spicer et al. 2007; Appelhans et al. 2012). All experimental animals showed quite stable pH-values over the duration of the NMR experiment, exemplified in fig. 18. As expected, $P(CO_2)_e$ was increased whenever $P(CO_2)_w$ was high (fig. 20A). Compensation for a (respiratory) acidosis was successful in all groups even under reduced availability of bicarbonate from the seawater. With the assumption of relatively high non-bicarbonate buffer values, the fact that $[HCO_3^-]_e$ is still elevated above the buffer line (fig. 21) underlines the contribution of ion exchange processes to acid-base regulation under hypercapnia. An increase of haemolymph bicarbonate at constant pH under hypercapnia could result from an uptake of bicarbonate from the seawater through Cl^-/HCO_3^- exchange or its formation due to excretion of protons or acid-equivalents to the seawater (such as NH_4^+; Fehsenfeld & Weihrauch 2013; Hans et al. 2014). After four weeks of incubation under moderately high $P(CO_2)_w$, the compensation of a respiratory acidosis seems to be more complete, compared to an acute exposure to 5700 ppm, where pH_e dropped to 7.6 (Truchot 1984). Even the uncompensated respiratory acidosis induced by an acute exposure to a reduction of $[HCO_3^-]_w$ at normocapnia (conditions of group 2; Truchot 1981; 1984) was not observed in this longer-term study. Confirmed by the present findings, increasing $[HCO_3^-]_e$ in response to hypercapnia prevails even after four weeks of exposure (comparing groups 1 and 3 in fig. 20; Truchot 1984). This indicates high capacities of the associated ion exchange mechanisms that contribute to pH-regulation over a longer period of time, and that they are largely unaffected by $[HCO_3^-]_w$.

All treatments with acidified seawater led to an increased cation concentration in the haemolymph, with significant increases of $[Mg^{2+}]$ and $[Na^+]$, comparable to findings in the Dungeness crab *Metacarcinus magister* (Hans et al. 2014) and the velvet crab *Necora puber* (Spicer

et al. 2007). The increase of $[Na^+]$ could indicate that pH_e regulation is at least in part contributed by the exchange of Na^+ to H^+ (see fig. 5) with an enhanced importance in mid-term responses to ocean acidification compared to acute responses. Increased $[Na^+]$ in the haemolymph can be achieved by an increase in the activity of the basolateral Na^+/K^+-ATPase in the gills, possibly contributing to the slightly increased energy demand and metabolic rates under simple hypercapnic conditions (group 1, fig. 14; Kreiß et al. 2015). However, it remains unclear why $\dot{M}O_2$ is depressed in the other groups, as these also show increased concentrations of Na^+ in their haemolymph and a similar degree of pH_e-regulation. The possibility of other – possibly neurological – responses interfering with the whole animal metabolic response and overshadowing the effects of systemic ion regulation is discussed below. As mentioned above, the fact that $[HCO_3^-]_e$ is still high in group 3 could be due to several factors in the excretion or uptake of acid-base equivalents. However, it might simply prove the high capacity of the bicarbonate uptake mechanisms such as the apical Cl^-/HCO_3^- antiporter in the gills. Maybe any uptake is not severely influenced by the availability of bicarbonate in the seawater because the reduction by 50% in this experiment was not big enough. Yet, even reductions in $[HCO_3^-]_w$ to one third of the initial alkalinity did not affect the accumulation of bicarbonate under acute exposure to hypercapnia (Truchot 1984). The stoichiometry of a shift in the activity of Na^+/H^+ exchange over Cl^-/HCO_3^- exchange in group 3 is not clearly quantifiable due to the large variation of the results of the ion chromatography on haemolymph samples. It was reported in fish gills that more extreme acidification enhances the activity of carbonic anhydrase and therefore enhances the formation of intracellular $[HCO_3^-]$. In this case, an uptake of bicarbonate is hindered, possibly favoring H^+ excretion to achieve acid-base regulation (Heuer & Grosell 2014). Such a process might be effective in *C. maenas* as well, especially under reduced $[HCO_3^-]_w$.

While all groups exposed to acidified water displayed an increase in cation concentrations, only group 3 also showed a non-significantly increased $[Cl^-]$. In group 2, $[Cl^-]$ was even significantly reduced, with a difference of about 110 mM between $[Na^+]$ and $[Cl^-]$ alone. Regarding this discrepancy between the two major ions (tab. 6; fig. 23) and the apparent the lack of negative charges from the absolute concentrations, it might be assumed, that a considerable amount of negative charges in the haemolymph has to be made up of either other non-carbonate anions, such as SO_4^{2-} or by negatively charged amino acids. But since chloride was the only anion quantified here, estimations have to be made carefully. A stronger gradient in chloride concentrations between haemolymph and seawater, as it was seen in groups 3 (tab. 6) could help in up-regulating $[HCO_3^-]_e$ and thus pH_e (Taylor 1977). The maintenance of a high-

er [Cl^-] in group 3 could possibly enhance the activity of the Cl^-/ HCO_3^- antiporter, leading to an increased outflow of Cl^- and a corresponding uptake of $[HCO_3^-]_e$, despite the reduced availability in the surrounding water. However, activity measurements of the individual transporters – desirably in relation to each other – are lacking. Again, high levels of haemolymph Cl^- may be achieved by an increased activity of the primary active, basolateral Na^+/K^+-ATPase and the secondary active, apical $Na^+/K^+/2Cl^-$ co-transporter. The reduced metabolic rates in group 3 compared to group 1 might indicate that this regulatory process may come at the expense of other energy consuming processes with the preference of acid-base regulation. This trait – and more specifically the reallocation of energy – seems to be triggered by the combined effects of high $P(CO_2)_w$ and low $[HCO_3^-]_w$, since the applied hypercapnic conditions alone (group 1) led to significantly higher SMR and RMR.

The significant difference of haemolymph [Cl^-] between groups 2 and 3 (fig. 23) could be related to different ways of how the internal acid-base balance is adjusted to ambient and haemolymph $P(CO_2)$. A respiratory acidosis during acute exposure to decreased seawater alkalinity at normocapnia (Truchot 1981; 1984) was not observed in this longer-term study (fig. 21). Truchot (1981; 1984) attributed his findings of elevated $P(CO_2)_e$ at low carbonate alkalinity to a retention of CO_2 in the crab due to a lesser CO_2 buffering capacity or capacitance coefficient $\beta(CO_2)_w$ under these conditions. Simply speaking, at high pH_w and normal alkalinity, more CO_2 can enter the seawater (e.g. during expiration), since a considerable amount is buffered by carbonate ions, according to the sum of formula [1] and [2] (for detailed reviews, see Dejours 1978 and Truchot & Forgue 1998):

$$CO_2 + H_2O + CO_3^{2-} \leftrightarrow 2\ HCO_3^- \qquad [12]$$

This change in the physico-chemical properties of the ambient water is still apparent in group 2, so maybe an effect of $\beta(CO_2)_w$ is not detrimental for $P(CO_2)_e$. Different ways to achieve pH_e regulation in the long run, dependent on the gradient between ambient and haemolymph $P(CO_2)$ may thus be active in the groups with reduced seawater bicarbonate, possibly involving different ion exchange mechanisms that lead to a significant difference in [Cl^-] between groups 2 and 3 (fig. 23). For the shore crab, further investigations on the activity of individual exchange processes across the gills should assess whether this hypothesis holds true. The difference in the capacitance coefficient $\beta(CO_2)_w$ brought by the change of seawater alkalinity is more pronounced at low than at high $P(CO_2)_w$ or pH_w (Dejours 1978; Truchot & Forgue 1998, see fig. A5 in the appendix). From this, Truchot (1984) concluded that acid-base regulation under elevated $P(CO_2)_e$ is simply independent of seawater alkalinity or $[HCO_3^-]_w$. This is con-

firmed by the similarity of the CO_2 parameters and pH_e values found between hypercapnic treatments, groups 1 and 3 (fig. 21). Future studies should take all parameters of the carbonate system into account when investigating the mechanisms involved in the physiological response to "ocean acidification".

Even though a significant increase in haemolymph $[Ca^{2+}]$ was found under hypercapnic conditions, its ratio to $[Na^{+}]$ was constant (fig. 22). A dissolution of the shell in order to increase the (bi-)carbonate concentration as a response to elevated $P(CO_2)_e$ was hypothesized for *Cancer productus* and is supported by concomitant increases of $[HCO_3^-]_e$ and $[Ca^{2+}]$ in its haemolymph (Defur et al. 1980). While the authors specify that the use of internal carbonate stores as source of buffers should be limited to acute responses to acid-base disturbances, they also suggest it to be a way to increase internal buffering capacities under conditions of reduced branchial function. It might be tempting to extend this thought to conditions of reduced availability of seawater bicarbonate, but the present data suggest that after four weeks, calcium concentrations – at least in relation to sodium – remain unchanged and that the elevated levels of $[HCO_3^-]_e$ are not originating from a dissolution of the shell. Any shell dissolution found in *C. maenas* may only be a transient way to regulate pH_e, so a time series of measurements would be necessary to investigate this.

It seems like *C. maenas* is able to tolerate disturbances in the ion homeostasis to a much higher degree than disturbances of the acid-base balance. While osmolarity of body fluids is the main factor to determine the cell volume, pH is crucial for optimal protein functioning and influence the oxygen affinity of haemocyanin (Truchot 1975; Whiteley et al. 2001). Moreover, pH_e can be seen as an intermediate to buffer pH_i against changes in ambient pH_w. Regulation of pH_e will eventually regulate pH_i and thus ensure optimal conditions of the cellular enzymatic activity. Electro-neutrality of the haemolymph and electrochemical gradients over cell membranes could be maintained by adjusting the distribution of negatively charged amino acids (glutamate and aspartate) and seems more likely than adjusting the activity of proteins to a new pH optimum. It has to be kept in mind, that through ion chromatography, only the concentration of fully dissociated ions was determined, neglecting differential ion-pair-formation and ion-activities *in vivo* (Cameron & Iwama 1989).

4.3 Influence on animal performance

Whether falling pH_e or pH_i might have a direct effect on whole-animal metabolic rates (Reipschläger & Pörtner 1996; Pörtner et al. 1998) cannot be concluded from the present data, as

no changes of pH were found across experimental groups (fig. 19) and no metabolic depression relative to control conditions was measured (fig. 14). Whilst the absolute difference between RMR and SMR (absolute routine aerobic scope) was significantly lower in group 3 than in all other treatments (fig. 15A), factorial routine aerobic scope was only slightly depressed in group 3 (fig. 15B). The proportional changes between SMR and RMR are quite constant among all groups. A relatively reduced routine aerobic scope indicates that activity is depressed or that less energy is available to be spontaneously spent on routine activity, possibly as a consequence of enhanced demands in acid-base or ion regulation (see above). Despite the insignificant changes of SMR and cardio-vascular activity between the experimental groups and the control group, the reduction of $[HCO_3^-]_w$ still significantly depressed the metabolic rates and blood flow rate compared to group 1 (fig 14 & 17B). These responses were the same, regardless of ambient $P(CO_2)_w$.

A strong similarity between SMR and blood flow rate can be seen across all groups, were group 1 tends to have the highest values and groups 2 and 3 have significantly lower metabolic rates and blood flow. However, no significant correlation between individual metabolic rates and blood flow was found (data not shown). Reduced flow rates under low $[HCO_3^-]_w$ could not be attributed to changes in heart rate, as it remained constant (fig. 17). Instead, the changes in the blood flow rate should result from a reduced stroke volume or contraction of the artery (Eckert et al. 2002). While these could not be accurately measured with the available equipment, it seems that the changes in metabolic rate are at least partly caused by corresponding changes in energy demand per heart stroke. Citing Taylor (1976) with heart rates nearly twice as high as those in the present study and determined at 15°C, he hardly found any changes of this parameter under hypoxia. Since no effect of the seawater carbonate system on heart rate could be found in the present study, it may thus be concluded that heart rate is neither affected by hypoxia nor hypercapnia. On the other hand, possible effects of the applied incubation parameters may be obliterated by the intermittent activity of the heart in *C. maenas* (Cumberlidge & Uglow 1977).

In line with recent findings for cod *Gadus morhua*, hypercapnia alone lead to slightly increased SMR, attributed to a higher activity in gill Na^+/K^+-ATPase (Kreiß et al. 2015) which would also explain the elevated of haemolymph $[Na^+]$ found here (fig. 23). However in *C. maenas*, a simultaneous increase of $P(CO_2)_w$ and reduction of $[HCO_3^-]_w$ also increased haemolymph $[Na^+]$ despite a significantly reduced SMR. Enhanced activity of gill Na^+/K^+-ATPase might thus be accompanied by a reallocation of energy away from various metabolic processes in other tissues whenever $[HCO_3^-]_w$ is reduced. This way, less blood has to pass

through these tissues, effectively leading to depressions in cardiac activity, itself then contributing to the reduced whole-animal metabolic rate.

pH_e was determined to be fairly constant under the given conditions, so changes in pH_i seem unlikely because pH_i is usually more tightly controlled than pH_e. The increase of $[HCO_3^-]_e$ in groups 1 and 3 is likely paralleled by an increase in bicarbonate in the intracellular compartment across all tissues (Heisler 1975). Despite constant pH values, an increased energy demand in internal ion regulation might contribute to the elevated $\dot{M}O_2$ in group 1, but does not explain the significant depression of SMR and RMR in group 3.

Changes in the haemolymph ion concentration (especially $[Mg^{2+}]$, tab. 5) are known to affect the oxygen affinity of haemocyanin (Truchot 1975). However, calculations of the P_{50} value have shown no significantly different effects in this experiment (see fig. A6 in the appendix). Obviously, the oxygen affinity is not compromised by the new steady-state in pH- and ion-regulation. Increases in haemolymph $[Mg^{2+}]$ are known to reduce activity in crustaceans and to aid in pH_i-regulation under abiotic stress (Sartoris & Pörtner 1997). Because $[Mg^{2+}]$ is elevated above control levels in all acidified incubations, differences in metabolic rates and blood flow cannot be attributed to the influence of extracellular $[Mg^{2+}]$ alone.

A reduced availability of bicarbonate to compensate for a hypercapnic acidosis might put an energetic strain on *C. maenas*, potentially reallocating energy between various energy consuming ion exchange processes and reducing the routine aerobic scope (fig. 15A). However, the original findings from Pörtner et al. (1998; 2000) suggest a reduced activity of Na^+/K^+-ATPase (driving apical Na^+/H^+ exchange), in favor of Cl^-/HCO_3^- exchange to be responsible for metabolic depression. With the recorded significantly elevated haemolymph $[Na^+]$, Na^+/K^+-ATPase and Na^+/H^+ exchanger might instead be of higher importance to regulate pH_e under hypercapnia and low seawater bicarbonate (cf. Kreiß et al. 2015). Based on the data presented in this study, changes in extracellular acid-base parameters in correspondence to the haemolymph ion composition cannot fully explain the observed pattern of oxygen uptake and blood flow rate.

4.4 Discussing possible CO_2-dependent signaling pathways affecting the metabolism

With similar values for pH_e, $P(CO_2)_e$ and $[HCO_3^-]_e$ in groups 1 and 3, none of the haemolymph acid-base parameters explains the significant differences in metabolic rates and blood flow rate between these two groups. The concentrations of cations in the haemolymph, while

being elevated above control levels, did not differ amongst experimental treatments (tab. 6; fig. 23). Their increase might be attributed to differentially increased efforts in ion and (non-respiratory) acid-base regulation. It has been measured in fish that decreases in blood plasma [Cl^-] (such as in group 2, fig. 22) and appropriate increases in [HCO_3^-] as a compensatory response to hypercapnia could alter the neuronal cell membrane ion gradient and thus their response during GABA binding (Heuer & Grosell 2014). Concomitantly, a local influence of the changes in haemolymph ion composition on neurons should not be completely neglected.

Seawater pH also does not hold as a trigger for the responses of the different groups: The values for pH_w in groups 2 and 3 differed the most (7.85 ± 0.05 and 7.19 ± 0.07, respectively), yet metabolic rates and blood flow were more similar in these two, compared to group 1 where the "intermediate" pH_w was 7.50 ± 0.03.

Changes on a cellular level at the direct interface between seawater and animal, namely the gills but also other epithelia, were not assessed here and are most likely involved in the transduction between the "detection" of seawater alkalinity and metabolic or cardiovascular responses (Henry et al. 2003; Perry & Abdallah 2012; Heuer & Grosell 2014, see below). Irrespective of pH_e, changes in pH_i of gill cells are likely, since they are facing the acidified seawater and will have different gradients in [H^+] towards the apical side. Even between different pairs of gills, a distinction regarding their specialization and share in acid-base regulation has to be made. While respiration and osmoregulation seem to be preferably divided between anterior and posterior gills, acid-base regulation is mediated by all pairs (Fehsenfeld & Weihrauch 2013). In any case, various signaling pathways could be localized in different gills and even a morphological restructuring of the gills under hypercapnia is conceivable (Fehsenfeld et al. 2011).

In a review on the physiological responses of fish to ocean acidification Heuer & Grosell (2014) suggest that the contact of sensory structures with seawater of altered $P(CO_2)_w$ may not instantly change the signal input. It may rather modify the organisms' responses on a longer timescale, possibly involving alternations of neuronal processes due to intracellular acid-base imbalances of sensory epithelia. Neuroepithelial cells acting as sensors for both seawater CO_2 and O_2 have been identified in zebra fish gills and are affected by changes of molecular CO_2, possibly mediated by changes in their pH_i (Perry & Abdallah 2012). The negative influence of hypercapnic seawater on chemo-reception in hermit crabs *Pagurus bernhardus* supports the idea of a direct interference of the seawater carbonate system with animal behavior (de la Haye et al. 2012). This might eventually also hold true for adaptations in oxy-

gen consumption (or general activity) and blood flow as found in the conditions of group 3 in this study. Considering the hyperpolarizing effect of reduced seawater [HCO_3^-] on neuroepithelial cells (Heuer & Grosell 2014) or simply the disturbance of the natural balance of CO_2-species, it seems likely that the excitation of the cells is affected by a changing speciation of CO_2 that effectively leads to different whole-animal responses. However, the presence of such cells has not yet been confirmed in marine crustaceans, especially those mediating a response directly linked to the cardiovascular system. In this context, the regulation and activity of membrane-bound and cytosolic carbonic anhydrase in the gills has to be considered as well, since its contribution to acid-base- and ion-regulation is evident (Henry et al. 2003; Heuer & Grosell 2014).

Increasing adenosine concentrations as a result of exceeding energy demand have a positive effect on cardiac performance, increasing heart rate and blood velocity in the sternal and posterior arteries in the lobster *Homarus americanus* (Stegen & Grieshaber 2001). The observed increase in the flow rate of group 1 (fig. 17B) may thus be intertwined with a metabolic increase of the haemolymph adenosine level. Adenosine in *Sipunculus nudus* was found to increase under hypercapnia and to be liable for the detected metabolic depression (see Pörtner et al. 2004), highlighting the diverse effects of this metabolite across animal species. As with adenosine, changes in the haemolymph concentration of lactate are known to cause behavioral and metabolic responses in crustaceans (De Wachter et al. 1997; Stegen & Grieshaber 2001). The quantification of metabolites with such a signaling function under the given experimental conditions could lead to additional interpretations of the presented data, especially concerning the way how environmental acid-base parameters are detected and affect the central nervous system directly. It has been shown for the toad *Bufo marinus* and postulated for *C. maenas*, that increasing levels of lactate increase $\dot{M}O_2$, involving catecholamines – a response blocked by adrenergic antagonists (Pörtner et al. 1994; De Wachter et al. 1997). While these responses are associated with hypoxia, signaling under hypercapnia might involve similar phenotypic effects.

The reduced metabolic capacities and blood flow found under reduced $[HCO_3^-]_w$ might be correlated with changes in the levels of specific hormones and neurotransmitters or the excitability of receptors to these transmitters. In this context, adenosine and ATP have been found to mediate hypercapnic acidification of the blood with reduced excitability in the central nervous system of vertebrates (Dulla et al. 2005) so the involvement of adenosine in the response to hypercapnia might be a fundamental trait. Whereas the Dungeness crab *Cancer*

magister only showed a transitory increase of lactate in its haemolymph as a response to hypercapnia (Pane & Barry 2007), lactate concentrations have been found to be elevated in the snail *Littorina littorea* after exposure to hypercapnia for one month. However, lactate remained at control levels if temperature was raised together with $P(CO_2)_w$ (Melatunan et al. 2011). This not only emphasizes interacting effects of changes in abiotic parameters, but also demonstrates that abiotic parameters can have antagonistic effects on the physiological response pattern. The present study can be used as a basis for further investigations expanding the scope of interactive effects, since here, antagonistic effects of elevated $P(CO_2)_w$ and reduced $[HCO_3^-]_w$ on oxygen uptake and blood flow have been shown.

4.5 Intraspecific variability in the ecophysiology of *C. maenas*

All animals used to evaluate the results in this work were males. From the random selection of animals then incubated, only one survivor was found to be female and it was incubated under high $P(CO_2)_w$ and low $[HCO_3^-]_w$ in group 3. It was not taken into the calculation of the means, because its specific response in some of the measured physiological parameters deviated considerably from the relatively uniform pattern of the males in group 3 (tab. 7). Special attention should be paid to the difference in SMR, which is twice as high in the female compared to the average of the males in this group, as well as to the relatively low pH_e of this animal. As a result of this pH value, $[HCO_3^-]_e$ was also very low at just 5.49 mM – a depression below control values (7.86 ± 1.05 mM). Ion concentrations appear to be unaffected, with the exception of $[Mg^{2+}]$. At 21 mM, this concentration is similar to control values. It should be kept in mind, that the data in tab. 7 are only based on the measurements in one female and have no statistical relevance. They might still show that sex-specific responses to the given experimental conditions should not be neglected in future studies.

Tab. 7. Comparison of the diverging parameters of average male and one female crab. The group averages are the mean values for group 3. The female crab was labeled "3.2". Only the values of diverging parameters are given, for those parameters missing, no apparent gender-specific difference was found.

Parameter	Unit	Group average	Female
SMR	nmol min^{-1} g^{-1}	9.17 ± 2.53	18.11 ± 1.34
RMR		27.66 ± 5.06	35.22 ± 1.40
pH_e	mM	7.79 ± 0.09	7.65 ± 0.08
$[HCO_3^-]_e$		11.33 ± 1.72	5.49
$[Mg^{2+}]$		32.0 ± 1.7	21.6

Aside from the possible sex-specific responses, no special attention was paid to the crabs' molting stage. Even though none of the crabs molted during their time at the institute (nine months from being caught until the end of the experiments), it cannot be concluded that molting was suppressed, since most of the animals used were in early intermolt. This was determined by their green coloring, along with their whitish integuments (McGaw et al. 1992). A few light-red crabs were included in the analysis, but they were the minority in all groups. Molt stage and thus coloring is supposed to have a striking effect on osmo- and oxyregulation, with red crabs, representing prolonged intermolt, being much less tolerant to low salinities and to hypoxia (Reid & Aldrich 1989; McGaw & Naylor 1992). These tolerance levels correlate with their ecology and there is a hypothesis that reduced tolerance to abiotic stressors is a trade-off to increase their mating success (Reid et al. 1997). The red crabs are more aggressive and have a higher $\dot{M}O_2$ under both "excited" and "rested" conditions than green crabs (Reid & Aldrich 1989; Kaiser et al. 1990). There is evidence that this trend exists within each group of this experiment, but the sample sizes are too small to develop any significant conclusion, also due to the fact that no comparative assay of the color forms was made here. Having a thicker carapace, a calculation of oxygen consumption in relation to fresh weight of the red crabs could thus be erroneous, whereas the weight specific oxygen demand of the tissue itself would be even greater (Reid et al. 1997).

The reduced capacities of osmoregulation in red crabs could very well be related to acid-base regulation and their responses to the selected experimental conditions. It would be advisable to differentiate more between the colorings of the animals in future experiments with the aim to identify the mechanisms that determine the observed physiological adaptations. In order to fully understand the effects of future ocean scenarios, including acidification, hypoxia and warming, clear distinctions between the responses of various color types and between genders should be considered. Whether combined changes in environmental factors favor the survival and reproduction success of one color variant over the other will provide important insight in the evolutionary future of the shore crab.

4.6 Perspectives

In the future, it will be interesting to analyze the remaining volume of the haemolymph samples for any changes in their metabolic profiles using ^{1}H- and ^{31}P-NMR spectrometry. Prolonged exposure to ocean acidification was shown to reduce the concentration of intracellular free amino acids, accompanied by an increased concentration of amino acids in the haemolymph (Hammer et al. 2012). Free amino acids as a major intracellular osmolyte (Charmantier

et al. 2009) might be quantified through NMR spectroscopy. According to the increase of extracellular cation levels, their redistribution between compartments may be necessary to balance not only the charges but also overall changes in osmolarity. Their fractional degradation may also introduce ammonia as a new way to excrete H^+ ions, similar to cytosolic pH-regulation under hypercapnia and reduced salinity (Fehsenfeld & Weihrauch 2013; Hans et al. 2014). If positively charged or uncharged amino acids were decomposed preferably over negatively charged ones, the detected changes in the number of charges could be balanced along with maintaining osmolarity.

It remains to be seen, if $P(CO_2)_w$, $[HCO_3^-]_w$ and pH_w have dose-dependent effects on the corresponding internal parameters (Walther et al. 2009; Thomsen & Melzner 2010). These might then have a detrimental effect on metabolic rate and cardiovascular activity. For *C. maenas*, reduced feeding rates, which might be another measure for energy demand, have only been found under more severe hypercapnia (3500 ppm), while pH_e was still fully compensated for (Appelhans et al. 2012). The interacting influences of temperature and hypoxia also need to be assessed in future studies, since these will be relevant in future oceans (see Walther et al. 2009; Deutsch et al. 2015). As mentioned above, changes in temperature together with $P(CO_2)_w$ have been shown to cause different responses of e.g. the oyster *Crassostrea gigas* (Lannig et al. 2010) and the snail *L. littorea* (Melatunan et al. 2011) compared to hypercapnia alone. In addition, ocean acidification narrows thermal tolerance windows in the spider crab *Hyas araneus* (Walther et al. 2009), which might also hold true for *C. maenas*. Adaptation to one abiotic driver might be compromised or aided by changes in another driver, thus calling for an integrative approach to predict whole animal responses to a changing marine environment (Melzner et al. 2013; Deutsch et al. 2015).

4.7 Conclusion

The shore crab *C. maenas* seems to be rather tolerant after one month of exposure towards the selected intensities of ocean acidification, which are well above the projected increases in seawater $P(CO_2)$ due to fossil fuel burning. Nevertheless, conditions such as those applied here can be found in upwelling areas (Gattuso et al. 2015). Control values of the observed parameters match those found in the literature, thus showing the suitability of the selected measurement setups. Extracellular pH-regulation under hypercapnia, leading to increased $P(CO_2)_e$ is effected by an active increase of $[HCO_3^-]_e$. This regulation was not influenced by the availability of bicarbonate from the seawater. All experimental changes in the seawater carbonate system seem to increase the concentration of inorganic ions in the blood, especially

[Na^+] and [Mg^{2+}]. Depending on the concentration of bicarbonate in the water, the standard metabolic rate was increased or depressed under hypercapnia. This trend was also visible in the blood flow rate, however the heart rate was not affected. From the performed whole-animal experiments and literature findings, a direct effect of the parameters of the seawater carbonate system on animal performance could be proposed that modulates the responses to ocean acidification. Further investigations will be necessary to identify sensory structures and signaling pathways. A control mediated through for example adenosine, other biogenic amines or hormones is suggested.

5. References

Ahsanullah M., Newell R. C. (1971): Factors affecting the heart rate of the shore crab *Carcinus maenas* (L.). *Comp. Biochem. Physiol*. 39A: 277-287.

Appelhans Y. S., Thomsen J., Pansch C., Melzner F., Wahl M. (2012): Sour times: seawater acidification effects on growth, feeding behavior and acid-base status of *Asterias rubens* and *Carcinus maenas*. *Mar. Ecol. Prog. Ser.* 459: 85-97.

Aronson R. B., Frederich M., Price R., Thatje S. (2014): Prospects for the return of shell-crushing crabs to Antarctica. *J. Biogeogr.* 1-7.

Belman B. W. (1975): Some Aspects of the Circulatory Physiology of the Spiny Lobster *Panulirus interruptus*. *Marine Biology*. 29: 295-305.

Boutilier R. G., Heming T. A., Iwama G. K. (1984): Appendix: physicochemical parameters for use in fish respiratory physiology. In: *Fish Physiology*, pp. 403-430. Ed. by Hoar W. S., Randall D. J., Academic Press, New York.

Brand M. D. (1990): The Contribution of the Leak of Protons Across the Mitochondrial Inner Membrane to Standard Metabolic Rate. *J. theor. Biol.* 145: 267-286.

Bryant D. J., Payne J. A., Firmin D. N., Longmore D. B. (1984): Measurement of Flow with NMR Imaging Using a Gradient Pulse and Phase Difference Technique. *Journal of Computer Assisted Tomography*. 8: 588-593.

Cameron J. N., Iwama G. K. (1989): Compromises between ionic regulation and acid-base regulation in aquatic animals. *Can. J. Zool*. 67: 3078-3084.

Charmantier G., Charmantier-Daures M., Towle D. (2009): Osmotic and Ionic Regulation in Aquatic Arthropods. In: *Osmotic and Ionic Regulation: Cells and Animals*, pp. 165-202. Ed. by Evans D. H., CRC Press, Boca Raton.

Crothers J. H. (1967): The Biology of the Shore Crab *Carcinus maenas* (L.). *Field Stud*. 2: 407-434.

Cumberlidge N., Uglow R. F. (1977): Heart and Scaphognathite Activity in the Shore Crab *Carcinus maenas* (L.). *J. Exp. Mar. Ecol*. 28: 87-107.

Dalla Via G. J. (1983): Bacterial Growth and Antibiotics in Animal Respirometry. In: *Polarographic Oxygen Sensors*, pp. 202-218. Ed. by Gnaiger E., Forstner H., Springer, Heidelberg.

De Graaf R. A. (2007): In vivo NMR spectroscopy: principles and techniques. 2nd Ed. Wiley VCH, Weinheim.

de la Haye K L., Spicer J. I., Widdicombe S., Briffa M. (2012): Reduced pH sea water disrupts chemoresponsive behavior in an intertidal crustacean. *J. Exp. Mar. Ecol.* 412: 134-140.

De Wachter B., Sartoris F. J., Pörtner H. O. (1997): The Anaerobic Endproduct Lactate has a Behavioural and Metabolic Signaling Function in the Shore Crab *Carcinus maenas*. *J. Exp. Biol*. 200: 1015-1024.

Defur P. L., Wilkes P. R. H., McMahon B. R. (1980): Non-Equilibrium Acid-Base Status in *C. productus*: Role of Exoskeletal Carbonate Buffers. *Respir. Physiol*. 42: 247-261.

Dejours P. (1975): Principles of Comparative Respiratory Physiology. North-Holland Publishing Company, Amsterdam.

Dejours P. (1978): Carbon Dioxide in Water- and Air-Breathers. *Respir. Physiol*. 33: 121-128.

Dejours P., Garey W. F., Rahn H. (1970): Comparison of ventilatory and circulation flow rates between animals in various physiological conditions. *Respir. Physiol*. 9: 108-117.

Deutsch C., Ferrel A., Seibl B., Pörtner H. O., Huey R. B. (2015): Climate change tightens a metabolic constrain on marine habitats. *Science*. 348: 1132-1135.

Dickson A. G. (1990): Standard potential of the reaction: AgCl(s) + ½ H_2 (g) = Ag(s) + HCI(aq), and the standard acidity constant of the ion HSO_4^- in synthetic sea water from 273.15 to 318.15 K. *Journal of Chemical Thermodynamics*. 22. 113-127.

Dogan F. (2011): Echtzeit MR-Bildgebung und Blutflussquantifizierung vom Herzen von Meeresorganismen. Diploma thesis, Hochschule Bremerhaven.

Doney S. C., Fabry V. J., Feely R. A., Kleypas J. A. (2009): Ocean Acidification: The Other CO_2 Problem. *Annu. Rev. Marine. Sci.* 1: 169-192.

Dulla C. G., Dobelis P., Pearson T., Frenguelli B. G., Staley K. J., Masino S. A. (2005): Adenosine and ATP Link *P*(CO_2) to Cortical Excitability via pH. *Neuron*. 48: 1011-1023.

Dupont-Prinet A., Chatain B., Grima L., Vandeputte M., Claireaux G., McKenzie D. J. (2010): Physiological mechanisms underlying a trade-off between growth rate and tolerance of feed deprivation in the European sea brass (*Dicentrarchus labrax*). *J. Exp. Biol*. 213, 1143-1152.

Eckert R., Randall D., Burggren W., Kathleen F. (2002): Tierphysiologie. Thieme, Stuttgart. pp. 585-655.

Fabry V. J., Seibel B. A., Feely R. A., Orr J. C. (2008): Impacts of ocean acidification on marine fauna and ecosystem processes. *ICES Journal of Marine Science*. 65: 414-432.

Fehsenfeld S., Weihrauch D. (2013): Differential acid-base regulation in various gills of the green crab *Carcinus maenas*: Effects of elevated environmental *p*CO_2. *Comp. Biochem. Physiol*. 164A: 54-65.

Fehsenfeld S., Kiko R., Appelhans Y. S., Towle D. W., Zimmer M., Melzner F. (2011): Effects of elevated seawater *p*CO_2 on gene expression patterns in the gills of the green crab, *Carcinus maenas*. *BMC Genomics*. 12: 488-504.

Fry F. E. J. (1971): The effect of environmental factors on the physiology of fish. *Fish physiology*. 6: 1-98.

Gatehouse P. D., Keegan J., Crowe L. A., Masood S., Mohiaddin R. H., Kreitner K. F., Firmin D. N. (2005): Applications of phase-contrast flow and velocity imaging in cardiovascular MRI. *Eur. Radiol*. 15: 2172-2184.

Gattuso J.-P., Magan A., Billé R., Cheung W. W. L., Howes E. L., Joos F., Allemand D., Bopp L., Cooley S. R., Eakin C. M., Hoegh-Guldberg O., Kelly R. P., Pörtner H.-O., Rogers A. D., Baxter J. M., Laffoley D., Osborn D., Rankovic A., Rochette J., Sumaila U. R., Treyer S., Turley C. (2015): Contrasting futures for ocean and society from different anthropogenic CO_2 emissions scenarios. *Science*. 349: aac4722.

Gillies R. J., Liu Z., Bhujwalla Z. (1994): ^{31}P-MRS measurements of extracellular pH of tumors using 3-aminopropylphosphonate. *American Journal of Physiology – Cell Physiology*. 267: 195-203.

Guppy M., Withers P. (1999): Metabolic depression in animals: physiological perspectives and biochemical generalizations. *Biol. Rev. Camb. Philos. Soc*. 71: 1-40.

Gutowska M. A., Pörtner H.-O., Melzner F. (2008): Growth and calcification in the cephalopod *Sepia officinalis* under elevated seawater pCO_2. *Mar. Ecol. Prog. Ser*. 373: 303-309.

Hammer K. M., Pedersen S. A., Størseth T. R. (2012): Elevated seawater levels of CO_2 change the metabolic fingerprint of tissues and hemolymph from the green shore crab *Carcinus maenas. Comp. Biochem. Physiol*. 7D: 292-302.

Hans S., Fehsenfeld S., Treberg J. R., Weihrauch D. (2014): Acid-base regulation in the Dungeness crab (*Metacarcinus magister*). *Mar. Biol.* 161: 1179-1193.

Heisler N. (1975): Intracellular pH of isolated rat diaphragm muscle with metabolic and respiratory changes of extracellular pH. *Respiration Physiology*. 23: 243-255.

Heisler N. (ed.) (1984): Acid-base regulation in animals. Elsevier, Amsterdam.

Henry R. P., Whaetly M. G. (1992): Interaction of Respiration, Ion Regulation and Acid-Base Balance in the Everyday Life of Aquatic Crustaceans. *Amer. Zool.* 32: 407-416.

Henry R. P., Gehnrich S., Weihrauch D., Towle D. W. (2003): Salinity-mediated carbonic anhydrase induction in the gills of the euryhaline green crab, *Carcinus maenas. Comp. Biochem. Physiol*. 136A: 243-258.

Heuer R. M., Grosell M. (2014): Physiological impacts of elevated carbon dioxide and ocean acidification on fish. *Am. J. Physiol. Regul. Integr. Comp. Physiol*. 307: R1061-R1084.

IPCC (2013): Climate Change 2013: The Physical Science Basis. Chapter 6: Carbon and other Biogeochemical Cycles. Contribution of Working Group I to the Fifth Assessment Report of the Intergovernmental Panel on Climate Change [Stocker T. F., D. Qin, G.-K. Plattner, M. Tignor, S. K. Allen, J. Boschung, A. Nauels, Y. Xia, V. Bex and P. M. Midgley (eds.)]. Cambridge University Press, Cambridge, United Kingdom and New York, NY, USA.

Ishimatsu A., Kikkawa T., Hayashi M., Lee K.-S., Kita J. (2004): Effects of CO_2 on Marine Fish: Larvae and Adults. *Journal of Oceanography*. 60: 731-741.

Johnson I., Uglow R. F. (1985): Some Effects of Aerial Exposure on the Respiratory Physiology and Blood Chemistry of *Carcinus maenas* (L.) and *Liocarcinus puber* (L.). *J. Exp. Mar. Biol. Ecol.* 94. 151-165.

Kaiser M. J., Hughes R. N., Reid D. G. (1990): Chelal morphometry, prey-size selection and aggressive competition in green and red forms of *Carcinus maenas* (L.). *J. Exp. Mar. Biol. Ecol.* 140: 121-134.

Klein Breteler W. C. M. (1975): Oxygen Consumption and Respiratory Levels of Juvenile Shore Crabs, *Carcinus maenas*, in Relation to Weight and Temperature. *Netherlands Journal of Sea Research*. 9: 243-254.

Kleps R. A., Myers T. C., Lipcius R. N., Henderson T. O. (2007): A Sex-Specific Metabolite Identified in a Marine Invertebrate Utilizing Phosphorus-31 Nuclear Magnetic Resonance. *PLoS ONE* 2(8): e780.

Kreiß C. M. (2010): Simultane Quantifizierung von extra- und intrazellulären pH-Werten bei *Carcinus maenas* unter CO_2-Einfluss mittels *in vivo* ^{31}P-NMR. Diploma thesis, University Bremen.

Kreiß C. M., Michael K., Lucassen M., Jutfelt F., Motyaka R., Dupont S. (2015): Ocean warming and acidification modulate energy budget and gill ion regulatory mechanisms in Atlantic cod (*Gadus morhua*). *J. Comp. Physiol. B.* DOI 10.1007/s00360-015-0923-7

Lannig G., Eilers S., Pörtner H. O., Sokolova I. M., Bock C. (2010): Impact of Ocean Acidification on Energy Metabolism of Oyster, *Crassostrea gigas* – Changes in Metabolic Pathways and Thermal Response. *Mar. Drugs*. 8: 2318-2339.

Linnaeus C. (1758): Systema Naturae per regna tria naturae, secundum classes, ordines, genera, species, cum characteribus, differentiis, synonymis, locis. *Editio decima, reformata. Laurentius Salvius: Holmiae.* ii, 824 pp.

McGaw I. J., Naylor E. (1992): Salinity preference of the shore crab *Carcinus maenas* in relation to coloration during intermoult and to prior acclimation. *J. Exp. Mar. Biol. Ecol*. 155: 145-159.

McGaw I. J., Kaiser M. J., Naylor E., Hughes R. N. (1992): Intrasepcific morphological variation related to the moult-cycle in colour forms of the shore crab *Carcinus maenas*. *J. Zool*. 228: 351-359.

Meinhausen M., Smith S. J., Calvin K., Daniel J. S., Kainuma M. L. T:, Lamarque J.-F., Matsumoto K., Montzka S. A., Raper S. C. B., Riahi K., Thomson A., Velders G. J. M., van Vuuren D. P. P. (2011): The RCP greenhouse gas concentrations and their extensions from 1765 to 2300. *Climate Change*. 109: 213-241.

Melatunan S., Calosi P., Rundle S. D., Moody A. J., Widdicombe S. (2011): Exposure to Elevated Temperature and $P(CO_2)$ Reduces Respiration Rate and Energy Status in the Periwinkle *Littorina littorea. Physiological and Biochemical Zoology*. 84: 583-594.

Melzner F., Gutowska M. A., Langenbuch M., Dupont S., Lucassen M., Thorndyke M. C., Bleich M., Pörtner H. O. (2009): Pysiological basis for high CO_2 tolerance in marine ectothermic animals: pre-adaptation through lifestyle and ontogeny. *Biogeosciences Discuss.* 6: 4693-4738.

Melzner F., Thomsen J., Koeve W., Oschlies A., Gutowska M. A., Bange H. W., Hansen H. P., Körtzinger A. (2013): Future ocean acidification will be amplified by hypoxia in coastal habitats. *Mar. Biol.* 160: 1875-1888.

Michaelidis B., Ouzounis C., Paleras A., Pörtner H. O. (2005): Effects of long-term moderate hypercapnia on acid-base balance and growth rate in marine mussels *Mytilus galloprovincialis. Mar. Ecol. Prog. Ser*. 293: 109-118.

Millero F. J. (2010): Carbonate constants for estuarine waters. *Marine and Freshwater Research*. 61: 139-142.

Moon R. B., Richards J. H. (1973): Determination of Intracellular pH by ^{31}P Magnetic Resonance. *The Journal of Biological Chemistry*. 248: 7276-7278.

National Exotic Marine and Estuarine Species Information System (NEMESIS). http://invasions.si.edu/nemesis/browseDB/SpeciesSummary.jsp?TSN=98734 on April 9th, 2015, 21:54.

Nobes C. D., Brown G. C., Olive P. N., Brand M. D. (1990): Non-ohmic proton conductance of the mitochondrial inner membrane in hepatocytes. *J. biol. Chem.* 265: 12903-12909.

Pane E. F., Barry J. P. (2007): Extracellular acid-base regulation during short-term hypercapnia is effective in a shallow-water crab, but ineffective in a deep-sea crab. *Mar. Ecol. Prog. Ser.* 334: 1-9.

Perry S. F., Abdallah S. (2012): Mechanisms and consequences of carbon dioxide sensing in fish. *Respiratory Physiology & Neurobiology*. 184: 309-315.

Pierrot D., Lewis E., Wallace D. W. R. (2006): MS Excel Program Developed for CO_2 System Calculations. ORNL/CDIAC-105a. Carbon Dioxide Information Analysis Center, Oak Ridge National Laboratory, U.S. Department of Energy, Oak Ridge, Tennessee. doi: 10.3334/CDIAC/otg.CO2SYS_XLS_CDIAC105a

Pörtner H. O., Boutilier R. G., Tang Y., Toews D. P. (1990): Determination of intracellular pH and P_{CO2} after metabolic inhibition by fluoride and nitrilotriacetic acid. *Respir. Physiol.* 81: 255-274.

Pörtner H. O., Branco L. G. S., Malvin G. M., Wood S. C. (1994): A new function for lactate in the toad *Bufo marinus. Journal of Applied Physiology*. 76: 2405-2410.

Pörtner H. O., Reipschläger A., Heisler N. (1998): Acid–base regulation, metabolism and energetics in *Sipunculus nudus* as a function of ambient carbon dioxide. *J. Exp. Biol.* 201: 43-55.

Pörtner H. O., Bock C., Reipschläger A. (2000): Modulation of the cost of pH_i regulation during metabolic depression: a ^{31}P NMR study in invertebrate (*Sipunculus nudus*) isolated muscle. *J. Exp. Biol.* 203: 2417–2428.

Pörtner H. O., Langenbuch M., Reipschläger A. (2004): Biological Impact of Elevated Ocean CO_2 Concentrations: Lessons from Animal Physiology and Earth History. *Journal of Oceanography*. 60: 705-718.

Reid D. G., Aldrich J. C. (1989): Variations in the response to environmental hypoxia of different colour forms of the shore crab, *Carcinus maenas. Comp. Biochem. Physiol*. 92A: 535-539.

Reid D. G., Abelló P., Kaiser M. J., Warman C. G. (1997): Carapace Colour, Inter-moult Duration and the Behavioural and Physiological Ecology of the Shore Crab *Carcinus maenas. Estuarine, Coastal and Shelf Science*. 44: 203-211.

Reipschläger A., Pörtner H. O. (1996): Metabolic depression during environmental stress: The role of extracellular versus intracellular pH in *Sipunculus nudus*. *J. Exp. Biol.* 199: 1801-1807.

Reipschläger A. G., Nilsson G. E., Pörtner H. O. (1997): Adenosine is a mediator of metabolic depression in the marine worm *Sipunculus nudus. Am. J. Physiol.* 272: R350-R356.

Riebesell U., Fabry V., Hansson L., Gattuso J.-P. (eds.) (2010): Guide to Best Practices for Ocean Acidification Research and Data Reporting. Publications Office of the European Union, Luxembourg.

Robertson R. F., Maegor J., Taylor E. W. (2002): Specific Dynamic Action in the Shore Crab, *Carcinus maenas* (L.), in Relation to Acclimation Temperature and to the Onset of the Emersion Response. *Physiological and Biochemical Zoology*. 75: 350-359.

Sabine C. L., Feely R. A. (2007): The Oceanic Sink for Carbon Dioxide. In Greenhouse Gas Sinks, D. Reay, N. Hewitt, J. Grace, and K. Smith (eds.), CABI Publishing, Cambridge, UK, pp. 31-49.

Sartoris F. J., Pörtner H. O. (1997): Increased concentrations of haemolymph Mg^{2+} protect intracellular pH and ATP levels during temperature stress and anoxia in the common shrimp *Crangon crangon*. *Journal of Experimental Biology*. 200: 785-792.

Siebers D., Lucu C., Böttcher K., Jürss K. (1994): Regulation of pH in the isolated perfused gills of the shore crab *Carcinus maenas J. Comp. Physiol. B.* 164: 16-22.

Small D., Calosi P., Whie D., Spicer J. I., Widdicombe S. (2010): Impact of medium-term exposure to CO_2 enriched seawater on the velvet swimming crab *Necora puber. Aquat. Biol*. 10: 11-21.

Steffensen J. F. (1989): Some errors in respirometry of aquatic breathers: how to avoid and correct for them. *Fish Pysiology and Biochemistry.* 6: 49-59.

Spicer J. I., Raffo A., Widdicombe S. (2007): Influence of CO_2-related seawater acidification on extracellular acid-base balance in the velvet swimming crab *Necora puber. Mar. Biol*. 151: 1117-1125.

Stapp L., Thomsen J., Melzner F., Schade H., Bock C., Pörtner H. O. (2014): Ocean acidification sensitivity of the Baltic blue mussel – variable phenotypic response within a population. Poster, SEB Annual Meeting 2014, Manchester.

Stegen E., Grieshaber M. K. (2001): Adenosine Increases Ventilation Rate, Cardiac Performance and Haemolymph Velocity in the American Lobster *Homarus americanus*. *Journal of Experimental Biology*. 204: 947-957.

Storch V., Welsch U. (2009): Kükenthal – Zoologisches Praktikum. Spektrum, Heidelberg. pp. 231-243.

Taylor A. C. (1976): The Respiratory Responses of *Carcinus maenas* to Declining Oxygen Tension. *J. Exp. Biol.* 65: 309-322.

Taylor A. C. (1977): The Respiratory Responses of *Carcinus maenas* (L.) to Changes in Environmental Salinity. *J. exp. mar. Biol. Ecol*. 29. 197-210.

Taylor E. W., Butler P. J. (1973): The behaviour and physiological responses of the shore crab *Carcinus maenas* during changes in environmental oxygen tension. *Netherlands Journal of Sea Research.* 7: 496-505.

Taylor E. W., Butler P. J. (1978): Aquatic and Aerial Respiration in the Shore Crab, *Carcinus maenas* (L.), Acclimated to 15°C. *J. Comp. Physiol*. 127: 315-323.

Taylor E. W.,Wheatly M. G. (1979): The Behaviour and Respiratory Physiology of the Shore Crab, *Carcinus maenas* (L.) at Moderately High Temperatures. *J. Comp. Physiol*. 130: 309-316.

Tepolt C. K., Somero G. N. (2014): Master of all trades: thermal acclimation and adaptation of cardiac function in a broadly distributed marine invasive species, the European green crab, *Carcinus maenas. J. Exp. Biol.* 217: 1129-1138.

Thomsen J., Melzner F. (2010): Moderate seawater acidification does not elicit long-term metabolic depression in the blue mussel *Mytilus edulis. Mar. Biol.* 157: 2667-2676.

Titulaer W. A. (1991): A respirometer of flexible design. *Comp. Biochem. Physiol*. 99A: 347-350.

Truchot J.-P. (1973): Temperature and acid-base regulation in the shore crab *Carcinus maenas* (L.). *Respiration Physiology*. 17: 11-20.

Truchot J.-P. (1975): Factors controlling the in vitro an in vivo oxygen affinity of the haemocyanin in the crab *Carcinus maenas* (L.). *Respiration Physiology*. 24: 173-189.

Truchot J.-P. (1976a): Carbon dioxide combining properties of the blood of the Shore Crab, *Carcinus maenas* (L.): CO_2-dissociation curves and haldane effect. *J. comp. Physiol*. 112: 283-293.

Truchot J.-P. (1976b): Carbon dioxide combining properties of the blood of the Shore Crab, *Carcinus maenas* (L.): Carbon dioxide solubility coefficient and carbonic acid dissociation constants. *J. exp. Biol.* 64:45-57.

Truchot J.-P. (1979): Mechanisms of the Compensation of Blood Respiratory Acid-Base Disturbances in the Shore Crab, *Carcinus maenas* (L.). *J. Exp. Zool.* 210: 407-416.

Truchot J.-P. (1981): The Effect of Water Salinity and Acid-Base State on the Blood Acid-Base Balance in the Euryhaline Crab, *Carcinus maenas* (L.). *Comp. Biochem. Physiol*. 68A: 555-561.

Truchot J.-P. (1984): Water carbonate alkalinity as a determinant of haemolymph acid-base balance in the shore crab, *Carcinus maenas*: a study at two different ambient $P(CO_2)$ and $P(O_2)$ levels. *J. Comp. Physiol. B*. 154: 601-606.

Truchot J. P., Forgue J. (1998): Effect of Water Alkalinity on Gill CO_2 Exchange and Internal $P(CO_2)$ in Aquatic Animals. *Comp. Biochem. Physiol*. 119A: 131-136.

Uglow R. F. (1973): Some effect of acute oxygen changes on heart and scaphognathite activity in some portunid crabs. *Neth. J. Sea Res*. 7: 447-454.

Uppström L. R. (1974): The boron/chlorinity ratio of deep-sea water from the Pacific Ocean. *Deep-Sea Research and Oceanographic Abstracts*. 21: 161-162.

Wallace J. C. (1972): Activity and Metabolic Rate in the Shore Crab, *Carcinus maenas* (L.). *Comp. Biochem. Physiol*. 41A: 523-533.

Walther K., Sartoris F. J., Bock C., Pörtner H. O. (2009): Impact of anthropogenic ocean acidification on thermal tolerance of the spider crab *Hyas araneus*. Biogeosciences. 6: 2207-2215.

Waters J. F., Millero F. J. (2013): The free proton concentration scale for seawater pH. *Marine Chemistry*. 149: 8-22.

Weihrauch D., Ziegler A., Siebers D., Towle D. W. (2001): Molecular characterization of V-type H^+-ATPase (B-subunit) in gills of euryhaline crabs and its physiological role in osmoregulatory ion uptake. *J. Exp. Biol*. 204: 25-37.

Wermter F. (2009): Entwicklung einer kontrastmittelgestützten *in vivo* ^{31}P-NMR Methode zur simultanen Quantifizierung von extra- und intrazellulären pH-Werten. Diploma thesis, Hochschule Bremerhaven.

Wermter F. (2012): Lokalisierte und bildgebende *in vivo* ^{31}P-NMR Spektroskopie an marinen Organismen. Master thesis, Hochschule Bremerhaven.

Whiteley N. M. (2011): Physiological and ecological responses of crustaceans to ocean acidification. *Mar. Ecol. Prog. Ser*. 430: 257-271.

Whiteley N. M., Scott J. L., Breeze S. J., McCann L. (2001): Effects of Water Salinity on Acid-Base Balance in Decapod Crustaceans. Journal of Experimental Biology. 204: 1003-1011.

Wittmann A. C. (2010): Life in cold oceans: activity dependent on extracellular ion regulation? Dissertation, University Bremen.

Wittmann A. C., Pörtner H. O. (2013): Sensitivities of extant animal taxa to ocean acidification. *Nature Climate Change*. 3: 995-1001.

Zange J., Grieshaber M. K., Jans A. W. H. (1990): The regulation of intracellular pH estimated by ^{31}P-NMR spectroscopy in the anterior byssus retractor muscle of *Mytilus edulis* L. *J Exp Biol*. 150: 95-109.

6. Appendix

6.1 Tables

Tab. A1. Measured fresh weight w_f and individual volume $V_{ind.}$ of five crabs to calculate the mean density factor *d*. Except for crab 5, none of these crabs were used in this study. Crab 5 was part of the control group.

Crab number	w_f	$V_{ind.}$	individual density
	g	mL	g/mL
1	65.2	72	0.9056
2	75.4	80	0.9425
3	29.06	37	0.7854
4	39.28	47	0.8357
5	46.95	54	0.8694
Mean density (*d*)			0.86772

Tab. A2. Actual composition of ions used to produce the carrier-solution for the 3-APP, determined by weight of the salts used.

Compound	MW	desired concentration	*m* for 100 mL	$m_{weighed}$	actual concentration
	g/mol	mM	mg	mg	mM
KCl	74.56	11.6	86.49	86.8	11.6
$CaCl_2 \bullet 2\ H_2O$	147.02	10.9	160.25	160.5	10.9
$MgSO_4 \bullet 7\ H_2O$	246.48	11.8	290.85	290.9	11.5
$MgCl_2 \bullet 6\ H_2O$	203.30	1.0	20.33	20.3	1.0
NaCl	58.44	415.5	2428.18	2428.3	415.5
NaOH	40.00	40.2	160.80	181.9	45.5

Tab. A3. Comparison of metabolic rates before and after the injection of 3-APP. Animals were taken from the control group and respiration rates were determined after the NMR experiments. Metabolic rates are given in nmol min^{-1} g^{-1}. Group means before the injection include all animals from the control group. Asterisks indicate whether the difference is significant (t-test, $P < 0.05$).

Animal	SMR before	SMR after	difference in means	RMR before	RMR after	difference in means
K1	10.02 ± 0.34	11.05 ± 0.17	1.03 *	39.59 ± 9.61	32.48 ± 12.51	- 7.11
K2	11.71 ± 0.37	11.73 ± 0.53	0.02	34.37 ± 5.59	49.45 ± 4.51	15.08 *
K9	11.11 ± 0.34	10.29 ± 0.21	- 0.82 *	39.97 ± 0.95	38.52 ± 4.97	- 1.45
group mean	10.55 ± 0.89	11.03 ± 0.72	0.47	40.67 ± 5.79	40.15 ± 8.60	0.52

6.2 Figures

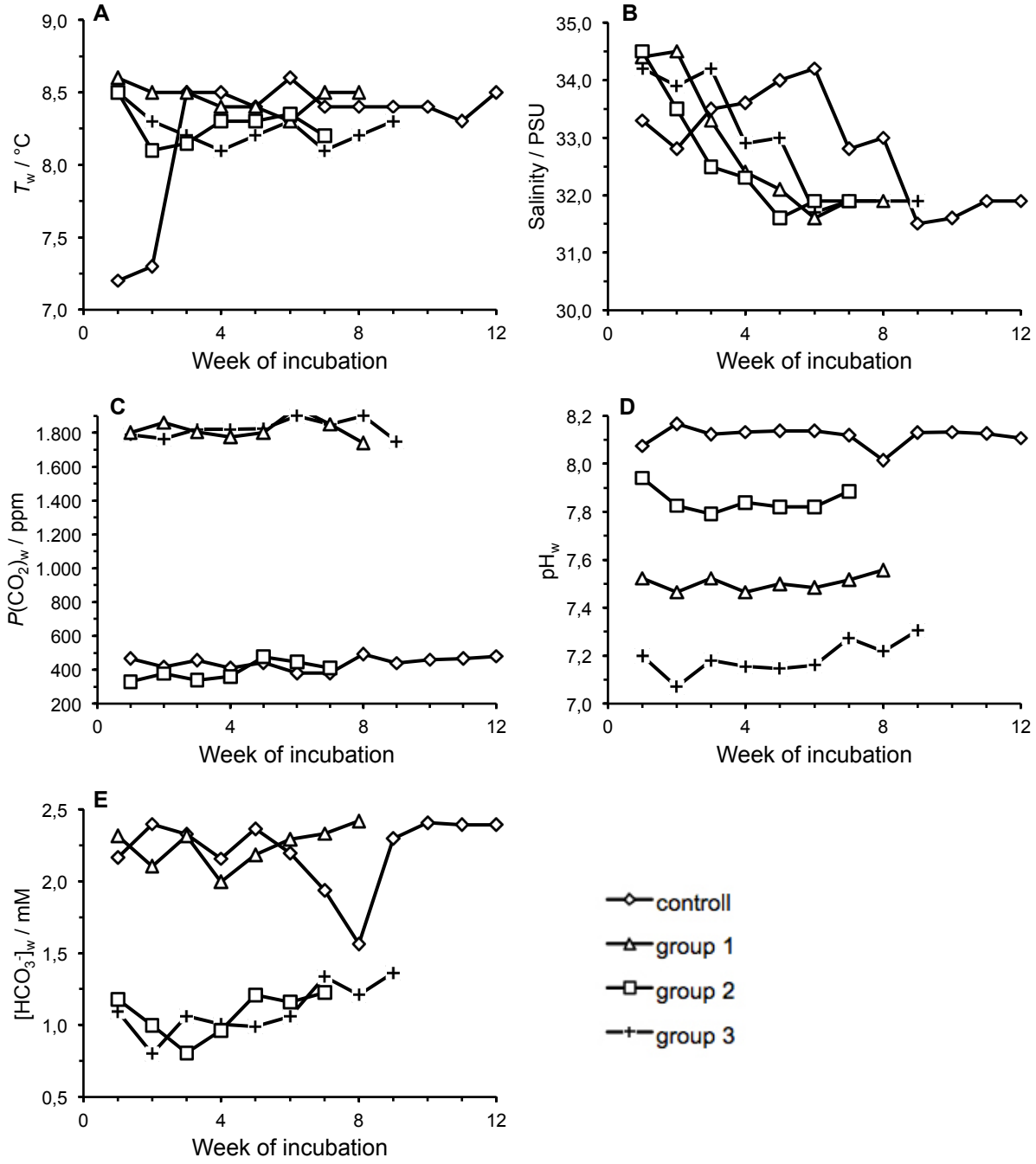

Fig. A1. Time series of seawater parameters during the incubation. A) Temperature; **B)** Salinity; **C)** $P(CO_2)$; **D)** Seawater pH on the free scale; **E)** $[HCO_3^-]_w$. Data points are mean values for the two incubation tanks. Measurements were scheduled once per week. Respiration measurements were conducted in the 5th week of incubation, followed by NMR-experiments in the 6th week. Haemolymph was sampled in the last week.

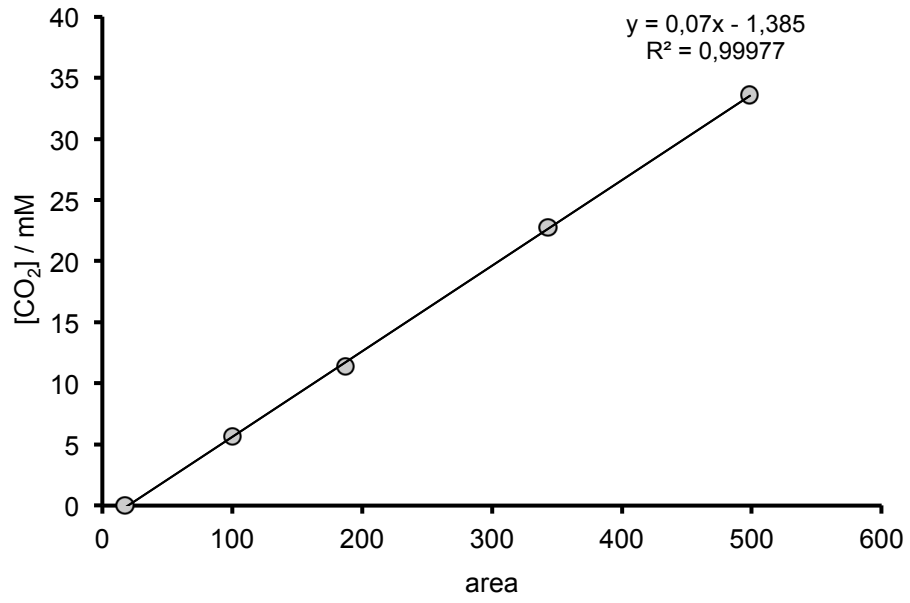

Fig. A2. Calibration curve for gas-phase chromatography. Data points represent the mean of a duplicate measurement. See *"2.5.1 Sampling and the carbonate system of the haemolymph"* for further details.

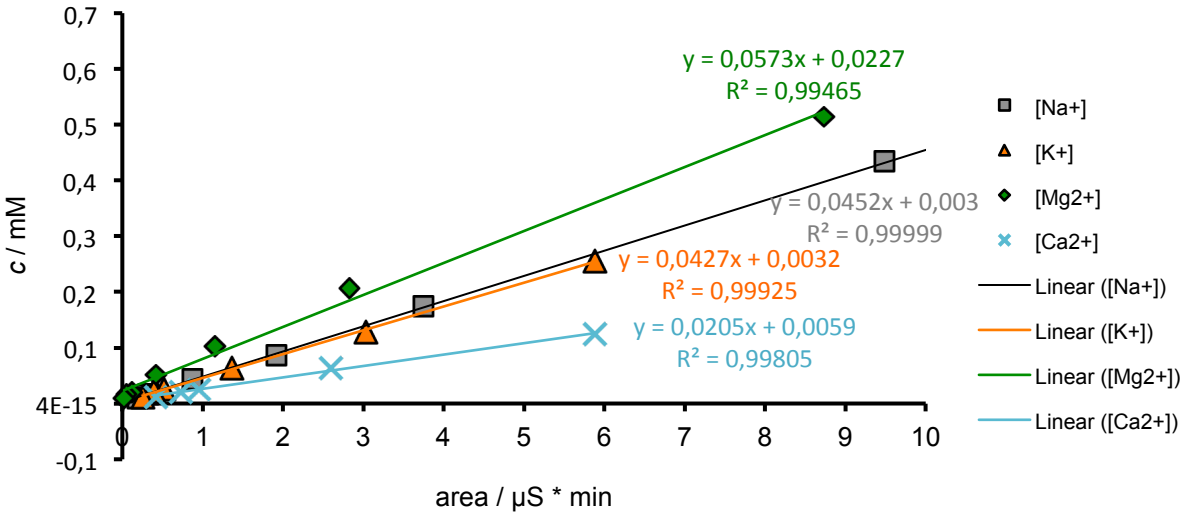

Fig. A3. Calibration curves for cations. Data points are derived from a single measurement at a given dissolution of the Dionex Combined Six Cation Standard-II. See *"2.5.Inorganic ion concentration"* for further details.

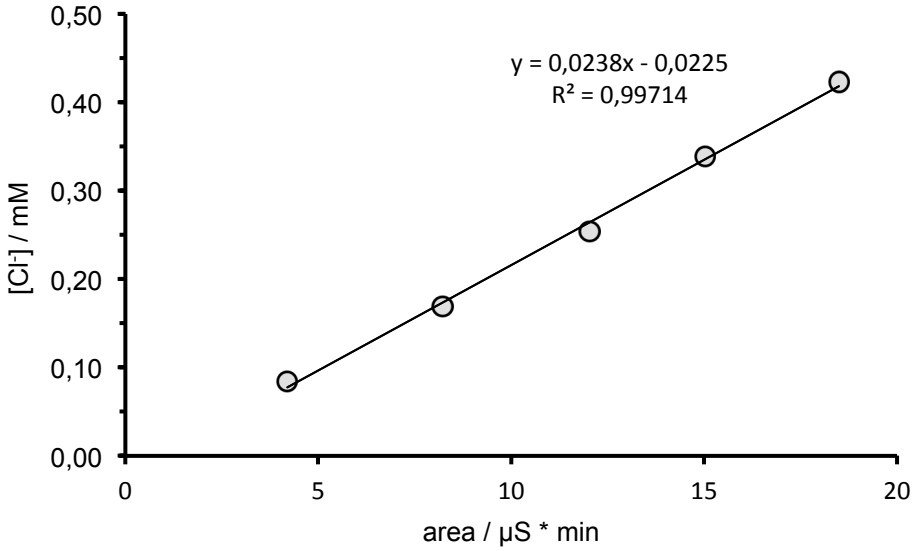

Fig. A4: Calibration curves for chloride. Data points are derived from a single measurement at a given dissolution of the Dionex Combined Five Anion Standard. See *"2.5.2 Inorganic ion concentration"* for further details.

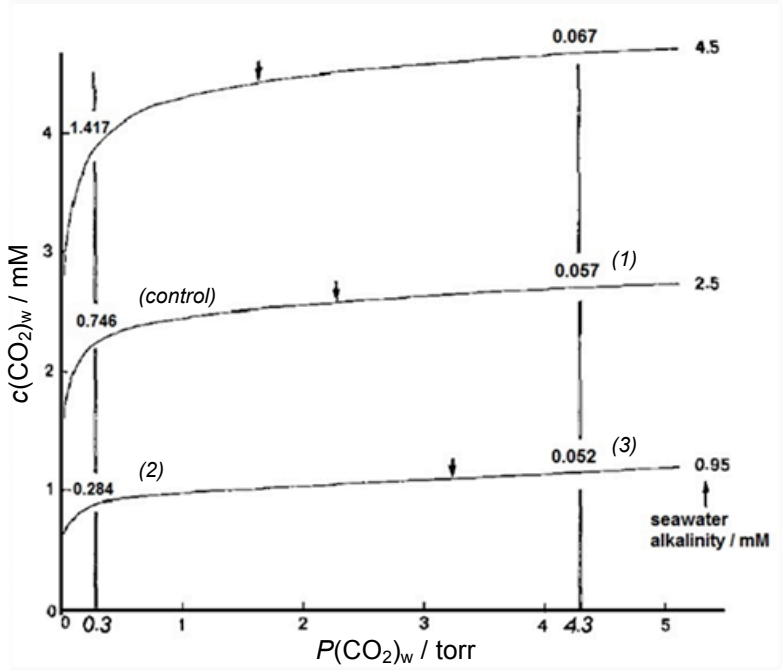

Fig. A5. Concentration of total CO_2 in natural seawater (S = 35; T = 15°C) of different alkalinities as a function of $P(CO_2)$. Alkalinity of 2.5 meq/L and $P(CO_2)_w$ of 0.3 can be seen as representative of control conditions. The CO_2 capacitance coefficient $\beta(CO_2)_w$ at a given $P(CO_2)$ and alkalinity can be estimated from the slope of the curve at that point. The numbers in brackets close to the respective values for $\beta(CO_2)_w$ stand for the approximate experimental conditions in this study. Note, how $\beta(CO_2)_w$ at the same $P(CO_2)$ differs under different alkalinities: Larger differences occur at low $P(CO_2)$, while at high $P(CO_2)$, the influence of alkalinity is negligible. Modified after Truchot (1984).

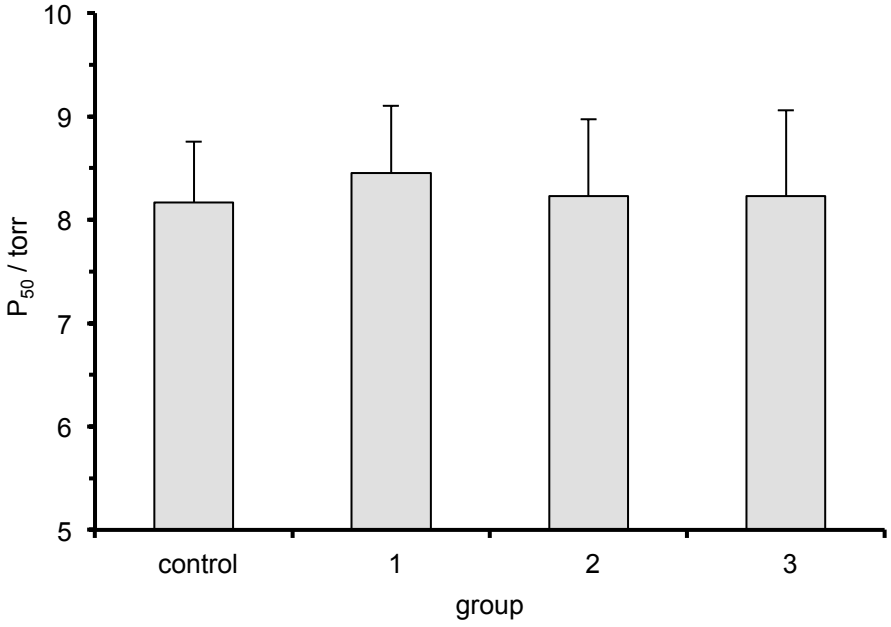

Fig. A6. Calculated P_{50} value of haemocyanin. A high value means oxygen is easily released. Data represents group means of individual calculations, based on Truchot (1975). The formula takes into account: T, $[Ca^{2+}]$, $[Mg^{2+}]$ and pH_e, which were measured in the present study.

6.3 Calculations

Calculating the volume of 25% HCl necessary to reduce the $[HCO_3^-]_w$ by 1.2 mM:

As 1 mol HCl (seen as equivalent to 1 mol H^+) transforms 1 mol HCO_3^- into H_2CO_3, the target concentration of HCl in the system of V_2 = 790 L sea water is c_2 = 1.2 mol/L.

c_{HCl} (25%) = 7.7139 mol/L

$$V_{HCl}\ (25\%) = \frac{c_2 \cdot V_2}{c_{HCl}} = \frac{1.2\,\frac{\text{mol}}{\text{L}} \cdot 790\ \text{L}}{7.7139\,\frac{\text{mol}}{\text{L}}} = 122.9\ \text{mL}$$

Accordingly, for 500 L sea water 77.78 mL 25% HCl were needed.

Calculation of α_{CO2}, pK_a''', $P(CO_2)_e$ and $[HCO_3^-]_e$ at the example of animal K1 (control group), according to Heisler (1986) and Pörtner et al. (1990):

Conditions:

T =	8°C
pH_e =	7.875
$c(CO_2)$ =	7.225 mM
$[Na^+]$ =	0.522 M
Ionic strength I =	0.66 M (Truchot 1976b)
Molarity of the haemolymph [M] =	1.1 M
Protein concentration [Pr] =	50 g/L (Robertston 1960)

$$\alpha_{\mathrm{CO_2}} = 0.1008 - 29.8 \cdot 10^{-3} \cdot [M] + (1.218 \cdot 10^{-3} \cdot [M] - 3.639 \cdot 10^{-3}) \cdot T - (19.57 \cdot 10^{-6} \cdot [M] - 69.59 \cdot 10^{-6}) \cdot T^2 + (71.71 \cdot 10^{-9} \cdot [M] - 559.6 \cdot 10^{-9}) \cdot T^3$$

$$\alpha_{\mathrm{K1}} = 0.1008 - 29.8 \cdot 10^{-3} \cdot 1.1 + (1.218 \cdot 10^{-3} \cdot 1.1 - 3.639 \cdot 10^{-3}) \cdot 8 - (19.57 \cdot 10^{-6} \cdot 1.1 - 69.59 \cdot 10^{-6}) \cdot 8^2 + (71.71 \cdot 10^{-9} \cdot 1.1 - 559.6 \cdot 10^{-9}) \cdot 8^3 = 0.0525 \frac{\mathrm{mM}}{\mathrm{torr}}$$

$$\mathrm{p}K_{\mathrm{a}}''' = 6.583 - 13.41 \cdot 10^{-3} \cdot T + 228.2 \cdot 10^{-6} \cdot T^2 - 1.516 \cdot 10^{-6} \cdot T^3 - 0.341 \cdot I^{0.323} - \log\left(1 + 0.00039 \cdot [\mathrm{Pr}] + 10^{(\mathrm{pH} - 10.64 + 0.011 \cdot T + 0.737 \cdot I^{0.323})} \cdot \left(1 + 10^{1.92 - 0.01 \cdot T - 0.737 \cdot T^{0.323} + \log\left([\mathrm{Na^+}] + (-494 \cdot I + 0.651) \cdot (1 + 0.0065 \cdot [\mathrm{Pr}])\right)}\right)\right)$$

$$\mathrm{p}K_{\mathrm{a}}'''_{\mathrm{K1}} = 6.583 - 13.41 \cdot 10^{-3} \cdot 8 + 228.2 \cdot 10^{-6} \cdot 8^2 - 1.516 \cdot 10^{-6} \cdot 8^3 - 0.341 \cdot 0.66^{0.323} - \log\left(1 + 0.00039 \cdot 50 + 10^{(7.875 - 10.64 + 0.011 \cdot 8 + 0.737 \cdot 0.66^{0.323})} \cdot \left(1 + 10^{1.92 - 0.01 \cdot 8 - 0.737 \cdot 8^{0.323} + \log\left(0.522 + (-494 \cdot 0.66 + 0.651) \cdot (1 + 0.0065 \cdot 50)\right)}\right)\right) = 6.124$$

$$P(\mathrm{CO_2})_{\mathrm{e}} = \frac{c(\mathrm{CO_2})}{10^{\mathrm{pH} - \mathrm{p}K_{\mathrm{a}}''' } \cdot \alpha + \alpha}$$

$$P(\mathrm{CO_2})_{\mathrm{e\,K1}} = \frac{7.225\ \mathrm{mM}}{10^{7.875 - 6.124} \cdot 0.0525 \frac{\mathrm{mM}}{\mathrm{torr}} + 0.0525 \frac{\mathrm{mM}}{\mathrm{torr}}} = 2.40\ \mathrm{torr}$$

$$[\mathrm{HCO_3^-}]_{\mathrm{e}} = P(\mathrm{CO_2})_{\mathrm{e}} \cdot \alpha \cdot 10^{(\mathrm{pH} - \mathrm{p}K_{\mathrm{a}}''')}$$

$$[\mathrm{HCO_3^-}]_{\mathrm{e\,K1}} = 2.40\ \mathrm{torr} \cdot 0.0525 \frac{\mathrm{mM}}{\mathrm{torr}} \cdot 10^{(7.875 - 6.124)} = 7.10\ \mathrm{mM}$$

Acknowledgements

First of all my thank goes to **Prof. Hans-Otto Pörtner** for giving me the opportunity to conduct this Master thesis under his supervision and at the laboratories of his section at the AWI. I also appreciate his initiative to help me with the interpretation of the data and getting the text in shape.

Secondly, to **Dr. Holger Auel** as my second supervisor on this thesis.

A very big thanks will have to be directed at **Dr. Christian Bock**, who diligently took the practical supervision of my work to his duties and without whom this thesis would never have been finished. Thank you for your patience, the helpful and countless advices and for the possibility to talk about all urgent news around the general subjects of "football" and "gaming".

I thank **Rolf Wittig** for his most valuable work on the automatic processing of the phosphorus NMR spectra and for answering all my questions revolving around the abstract nature of nuclear magnetic resonance.

I would like to say thanks to **Dr. Astrid Wittmann**, **Dr. Franz Sartoris** and the technical staff of the section of integrative ecophysiology, namely **Fredy Véliz Moraleda**, **Silvia Hardenberg**, **Timo Hirse**, **Nils Koschnick** and **Isabell Ketelsen** for their help and initiative to introduce me to the various apparatuses that I used in my work and for their help with the incubation setup and maintenance. Thanks also to **Kai Wätjen**, who brought the crabs to the institute.

Thank you **Sarah**, **Berit** and **Anja** for your help on the haemolymph sampling and making me feel like the head of a research group for half a day.

Also to the other Bachelor and PhD students at the IEP section, namely **Matze**, **Feli**, **Steffen**, **Miguel** for being such a great company. A general thanks to all the ecophysiologists at the AWI for making up a really fun working atmosphere and for always being helpful.

Last but far from least, to Mama, Franzi and Nina, the rest of my family and all my friends near and far, without whom I would never have been able to have done this: Thank you!

I dedicate this work to my father, who sadly passed away before seeing me finish it.

Declaration

I hereby assert that this thesis at hand is in all parts my own work. Only the quoted sources and references have been used. Any direct or indirect adaptation of the work of others has been marked and referred to as such. This thesis has not been submitted in the same or similar version, not even in part, to any other authority for grading and has not been published elsewhere.

_____

Bastian Maus

Bremen, the 9th of September 2015